

Geology and Mineralization of the Hoodoo Mountain Area (NTS 104B/14E)

by M.G. Mihalynuk, J.M. Logan, A. Zagorevski¹ and N. Joyce¹

KEYWORDS: Hoodoo Mountain, Andrei Icefield, volcanic-hosted massive sulphide, Rock and Roll, copper porphyry, Galore Creek, Stikine assemblage, Stuhini Group, Iskut River, Twin Glacier River, Bronson

INTRODUCTION

The Iskut River area of northwestern British Columbia is characterized by exceptional mineral endowment. A 20 km-wide corridor south of the Iskut River includes the Bronson Slope, Snip, Johnny Mountain, Eskay Creek and Rock and Roll deposits with past production or defined resources (Figure 1). These deposits formed in a surprisingly diverse set of environments ranging from intrusion hosted sulphide veins to shallow subaqueous hot spring settings. No deposits with past production or defined resources occur within a 20 km corridor immediately north of the Iskut River, yet those farther afield include Galore Creek, Copper Canyon and Schaft Creek deposits that are hosted by alkalic and calcalkalic porphyries. An obvious explanation for the dearth of deposits within the northern corridor is not forthcoming from existing geological maps; however, a significant part of the corridor has either never been systematically mapped or at least not since it was surveyed by Forrest Kerr in the 1920s. A working partnership was established between the British Columbia Ministry of Energy, Mines and Petroleum Resources, the Geological Survey of Canada (under the auspices of the Geoscience for Energy and Minerals Strategy: GEMS), Pacific North West Capital Corp., and the University of Victoria to address this lack of public geologic knowledge through systematic mapping. Supplementary goals were to provide a more accurate geological setting for the Rock and Roll deposit and to evaluate the potential for similar precious metal rich polymetallic massive sulphide mineralization within the Iskut and adjacent regions (Figure 1). Our work was mainly focused where published mapping was entirely lacking: the eastern half of the Hoodoo Mountain map

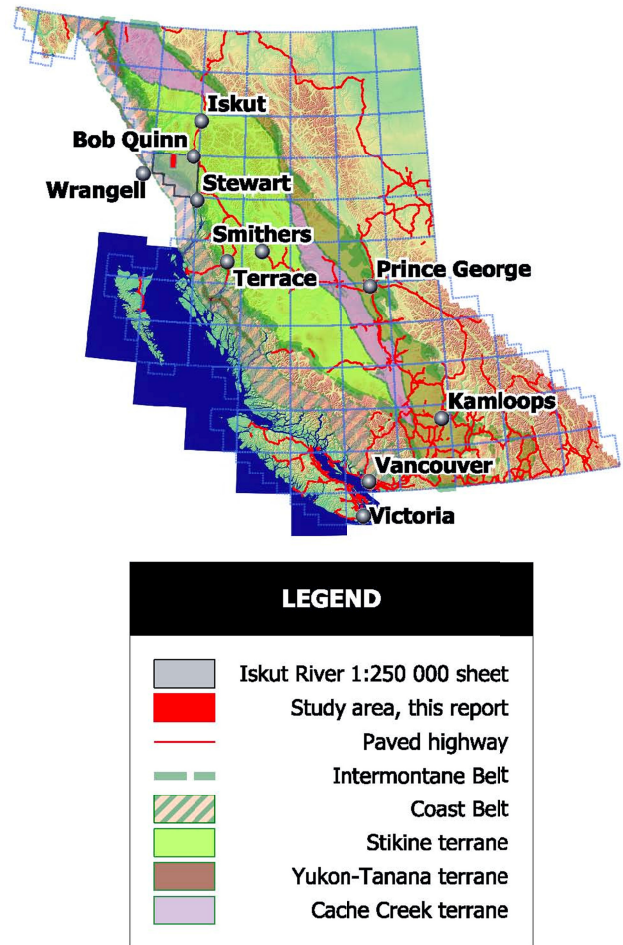


Figure 1. Location of the Iskut study area near the boundary of the Coast Belt and western Stikine terrane.

sheet (NTS 104B/14E, Figures 2 and 3). This map sheet is bordered to the north by the Galore Creek map sheet (104G/03; Figure 2) and to the east by Forrest Kerr map sheet (104B/15), both covered by relatively recent regional geological surveys (Logan and Koyanagi, 1994, 104G/03, 04; and Logan *et al.*, 2000, 104B/10, 15, 104G/02, 07W; Figure 2).

LOCATION AND ACCESS

Access to the Hoodoo Mountain map area (NTS 104B/14E) is via the Bronson airstrip, located along the Iskut River 300 km north-northwest of Terrace, 330 km northwest of Smithers, and 75 km east-northeast of

¹ Geological Survey of Canada, Natural Resources Canada, Ottawa, ON

This publication is also available, free of charge, as colour digital files in Adobe Acrobat® PDF format from the BC Ministry of Forests, Mines and Lands website at <http://www.empr.gov.bc.ca/Mining/Geoscience/PublicationsCatalogue/Fieldwork>.

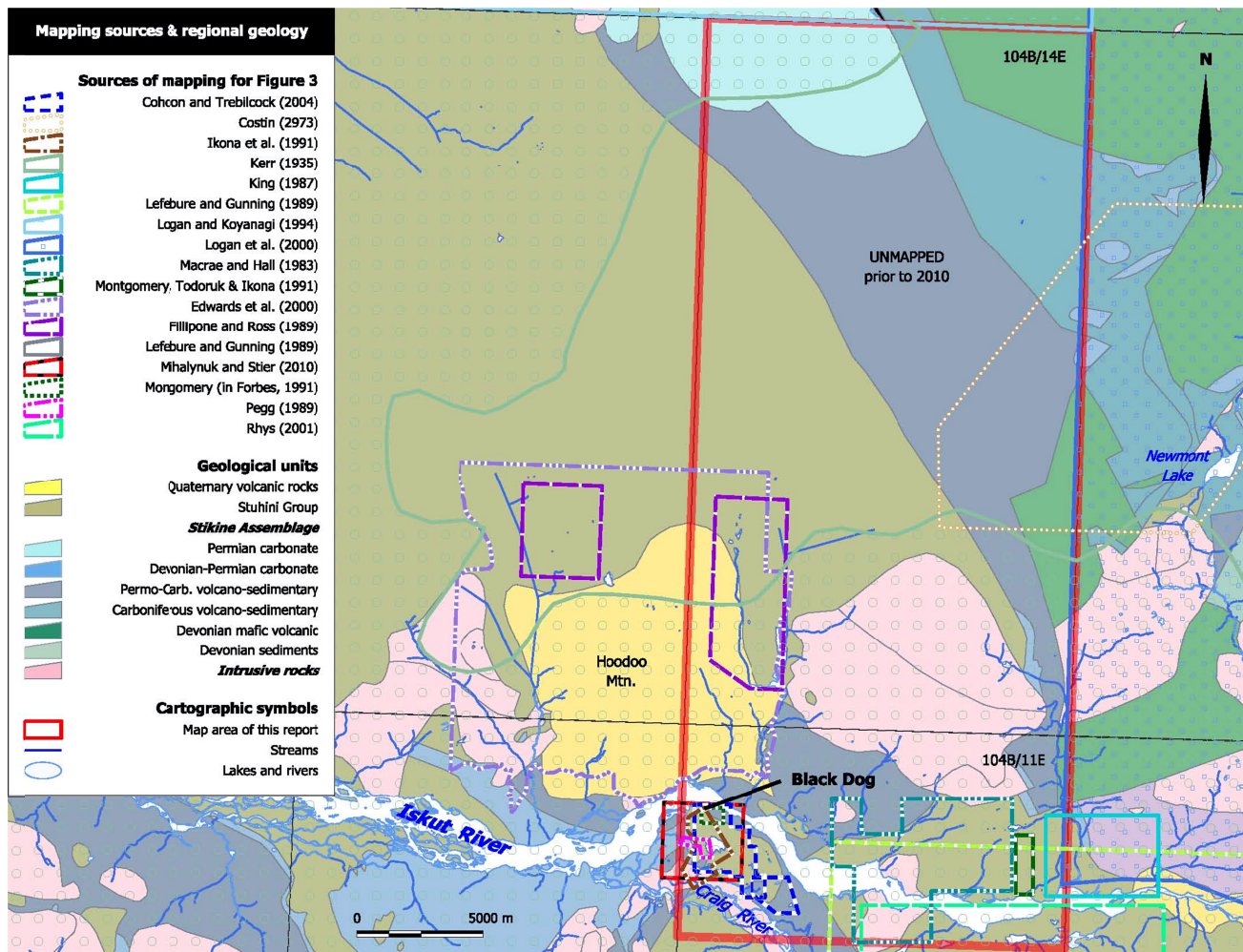


Figure 2. Sources of geological map information within the area between the Craig River and the eastern Hoodoo Mountain map sheet (NTS 104B/14W). Location of the Rock and Roll property (Black Dog surface showing) and important landmarks are also indicated. The regional geology portrayed within the study area (red rectangle) is largely after Kerr (1935) as compiled by (Massey *et al.*, 2005).

Wrangell, Alaska (Figure 1). Both Terrace and Smithers are serviced by scheduled commercial flights from Vancouver and both are approximately 400 km by road (~5 hour drive) from Bob Quinn airstrip. Bronson airstrip is a 60 km flight southwest from Bob Quinn, the nearest airstrip that is serviced by road access. Seasonal charter helicopter service is generally available from Bob Quinn. The nearest permanent charter helicopter base is in Stewart, approximately 110 km to the southeast. In 2010, two seasonal camps adjacent to the airstrip were in operation. Accommodations could be arranged at the Skyline Gold Corp. or the Kossey fishing camp on the Iskut River.

Iskut River occupies a U-shaped glacial valley with alpine glaciers draping many of the adjacent ridges and extending to well below treeline at ~1000 m elevation. Our fieldwork focused on the mountain slopes north of the Iskut River and nunataks of the Andrei Icefield and its distributary glaciers. (Note that herein we refer to the Andrei Icefield as the collective ice mass and high névé/accumulation zone from which the many large

valley glaciers of the area emanate. The Andrei Glacier we refer to as the main, >2 km wide, outflow glacier in the northeast corner of 104B/14 (Figure 3) the terminus of which is 10.5 km north-northeast of Newmont Lake in 104B/15; Figure 2). Work in this typically rainy coastal region is commonly curtailed by low cloud and inability to fly; however, mid-August of 2010 was uncharacteristically warm and cloud-free. Our work was also facilitated by the well-appointed Skyline Gold Corp. base camp at Bronson airstrip and helicopter accompaniment of VIH Helicopters Ltd.

REGIONAL GEOLOGY AND PREVIOUS WORK

Most rocks north of the Iskut River within NTS 104B/14E have not been mapped as part of a systematic regional program. Topographical mapping by the International Boundary Commission with additions by Forrest Kerr between 1926 and 1929 (Kerr, 1948; Figure 2) covered the corridor along the Iskut River, but Kerr

Layered Rocks

Quaternary

Hoodoo volcanic complex

Early Jurassic

well-bedded green lapilli-ash tuff
maroon ash tuff/tuffite, also in

Late Triassic and Carboniferous

hornblende-biotite ash flow ~187Ma

Late Triassic

orange wacke ± biotite/K-feldspar

well-bedded wacke ± chert clasts

dacite ash flow ~220 Ma

polymictic conglomerate

feldspar pyroxene breccia ± pillowed

Middle-Late Triassic

rusty graphitic argillite/siltstone

Paleozoic - Triassic

quartz sandstone

siltstone ± volcanic / laminated

chert (also Carboniferous-Permian)

carbonaceous siltstone

tuffaceous Phyllite/wacke

andesite breccia and lesser ash

mafic volcanic - tuff and minor flow

sericite schist

undivided sediment/volcanic

felsic tuff and minor flows

ash flow in Carboniferous

argillite > volcanic sediment/tuff

turbiditic, also Carboniferous

Early Permian

limestone -massive to well-bedded

marble (± Carboniferous)

Carboniferous

tuffite with chert/exhalite

volcanic wacke/conglomerate

limestone, commonly crinoidal

basalt -pillowed and breccia

Intrusive Rocks

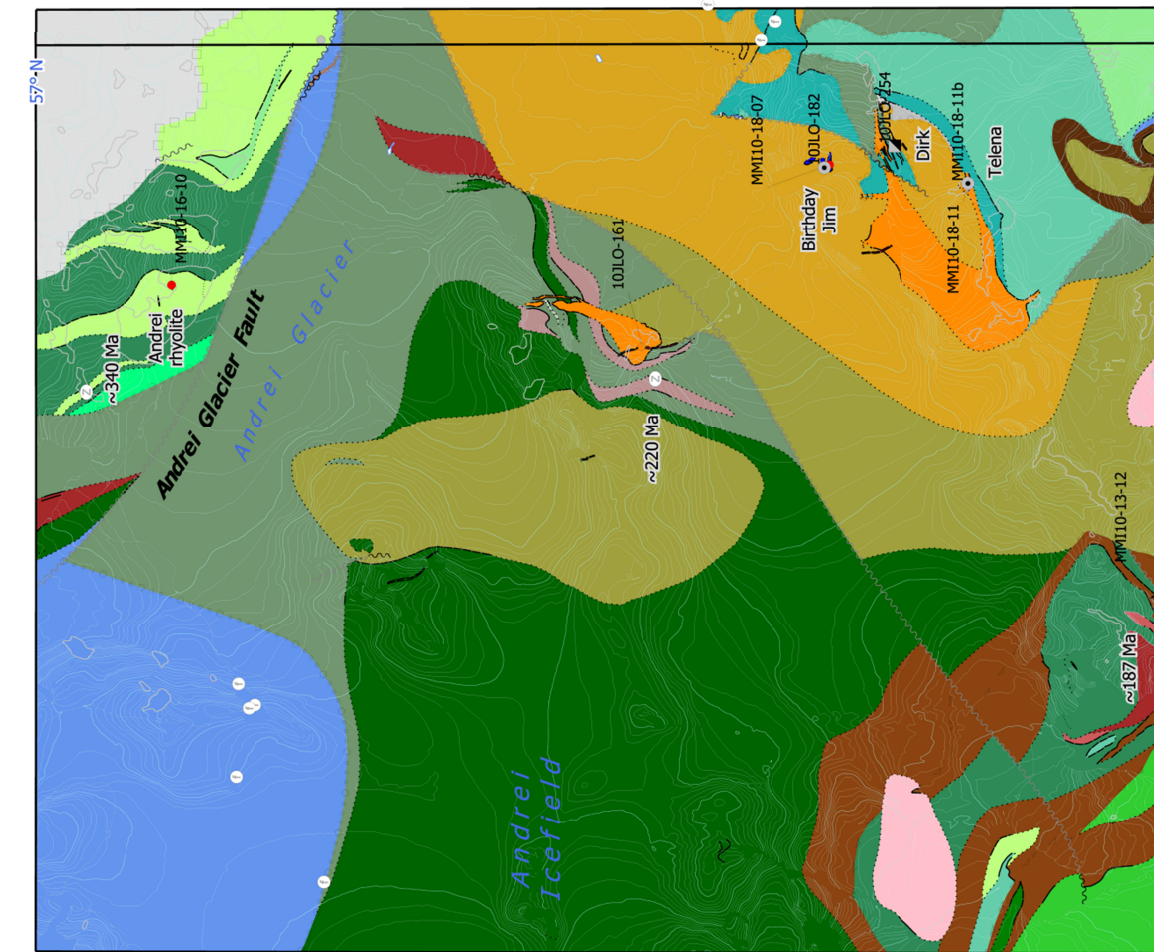
Eocene

Early? Eocene granodiorite

Jurassic-Eocene quartz diorite

Early to Middle Jurassic

granodiorite, diorite, undivided



designated the area farther north as one “Large ice field with a few peaks rising above the ice level”. Indeed, in the 1920s much more of the region was covered by ice than is today. A striking example of glacial retreat can be seen at Twin Glacier (Figure 4). When Kerr surveyed and mapped this area, two tongues of ice surrounded a 5 km long nunatak east of Hoodoo Mountain, re-joining and extending about 1 km south of the nunatak as shown on his 1:126 720 scale map. By the time aerial surveys were conducted in the mid 1970s for the National Topographic 1:50 000 scale Mapping program, the glacier had melted back to form two separate tongues with a kilometre of the eastern tongue replaced by a lake. Provincial aerial surveys in the late 1980s produced the base for the 1:20 000 scale Terrain Resource Information Management (TRIM) maps, at which time the lake had grown to 2 km in length, with the ice having melted back an additional 1 km. High resolution satellite imagery captured in October, 2010 show the terminus of the eastern tongue having retreated an additional 1.7 km. Thus, much of Kerr’s “Large Ice fields...” terrain is now exposed and never-before-seen rock exposures are everywhere, including new outcrops with significant mineralization.

Subsequent mapping in the area covered the southwest corner of 104B/14E as part of a study of the Holocene Hoodoo Mountain volcanic rocks (Edwards *et al.*, 2000) and a structural study focused in part on the Twin Glacier nunatak (Fillipone and Ross, 1989). Many parts of the Iskut map area (1:250 000 scale, NTS 104B) were mapped as part of Geological Survey of Canada program under the direction of Anderson in 1991 (Anderson, 1993), but persistently inclement weather prevented systematic coverage in the area around the Andrei icefield in 104B/14E (Anderson, personal communication, 2010). Mihalynuk *et al.* (2010) provides an overview of other geological studies in the Iskut region, which is not repeated here.

Existing maps of 104B/14E separate the Mesozoic and older strata into two domains: an eastern domain underlain primarily by Paleozoic Stikine assemblage (Monger, 1977) and a western domain underlain by volcanic and derived sedimentary rocks of the Stuhini Group (Souther, 1971). Our work in 104B/14E extends the geological relationships most recently outlined by Logan *et al.* (2000) in the adjoining map sheets to the east and north. Preliminary interpretation of the geological data collected in 2010 indicates that the Late Triassic



Figure 4. A view to the south of the eastern lobe of the Twin Glacier showing drastic retreat since ca. 1920. The ridge on the west side of the photo formed an isolated nunatak in the 1920s. This photo was taken at the end of a heat wave in August of 2010.

Stuhini Group arc and basal strata form a belt that broadens westward where it is overlain by Early Jurassic volcanic strata (Figure 3). Stuhini Group unconformably overlies a composite basement of deformed, Carboniferous (to Devonian (?)) and Late Paleozoic volcanic arc and carbonate bank deposits of the Stikine assemblage (Brown *et al.*, 1991).

East-directed thrust faults interleave and duplicate Paleozoic and Mesozoic strata. High angle faults dissect the thrust faulted terrain and have subsequently been cut by intrusions that are Mesozoic to Eocene in age. Two main periods of mineralization are recognized: Carboniferous, volcanogenic massive sulphide-style and probable Late Triassic age (Bernales *et al.*, 2008) intrusion-related vein, skarn and disseminated mineralization. Details of the stratigraphy, structural disruption, intrusion and mineralization follow.

STRATIGRAPHY

Stratigraphic assignments rely on the work in adjacent areas, particularly the work of Logan *et al.* (2000), which builds upon extensive fossil collections and isotopic age data. Three well dated and easily recognizable stratigraphic intervals form the framework for stratigraphic correlations within the Hoodoo Mountain area. Two of these intervals, Carboniferous and Permian, contain distinctive thick carbonate units. Carboniferous carbonate is characterized by abundant large crinoid columnals (Figure 5). Permian carbonate is recognized by the presence of large Rugosan horn corals (Figure 6a), and locally, by accumulations of giant foraminifera (Figure 6b). A third interval, dominated by brown and orange weathering, coarse biotite and K-feldspar-phyric tuff and volcanogenic conglomerate, is believed to be of Late Triassic age (see below). Other conglomerate units are less diagnostic and likely range from Devonian to Jurassic in age.



Figure 5. Packstone dominated by crinoid columns in the eastern Hoodoo Mountain area. Large crinoid columns are characteristic of the Carboniferous limestone strata.



Figure 6a. Characteristic Permian fossils within the Hoodoo Mountain area; Rugosan horn corals.



Figure 6b. Characteristic Permian fossils within the Hoodoo Mountain area; giant fusulinaceans (2 cm long) in a packstone.

Devonian

Lower to Middle Devonian strata are recognized in the Forrest Kerr area as “...penetratively deformed, intermediate to mafic metavolcanic tuff, flows, diorite and gabbro, recrystallized limestone, graphitic schist and quartz sericite schist...” (page 12, Logan *et al.*, 2000). Devonian rocks have not been positively identified within the eastern Hoodoo Mountain area; however, isolated outcrops of marble and mafic meta-igneous rocks immediately west of the Bronson airstrip may belong to this old rock package. In addition, an undated sequence of mafic to intermediate volcanoclastic rocks, tuff, graphitic phyllite, slate and limestone intruded by metagabbro

plugs and basic dikes underlie the Twin Glacier nunatak. The lithological associations, poly-phase deformation and metamorphism resemble those of Devonian strata elsewhere (Logan *et al.*, 2000). However, the lack of concrete age control for these rocks does not preclude the originally suggested Triassic age (Kerr, 1948).

Carboniferous

Strata of Carboniferous age are extensively exposed in the eastern Hoodoo Mountain area. They include bimodal mafic and felsic volcanic rocks and intervals of well-bedded carbonate, chert and wacke. Similar volcanic rocks in the Forrest Kerr area display primitive arc characteristics (Logan *et al.*, 2000) and are associated with VHMS Zn-Pb-Cu ±Ag-Au mineralization (Logan, 2004). Carbonate and other sediment-dominated strata overlie the Carboniferous volcanic sequence.

Mafic volcanic rocks

Carboniferous mafic volcanic rocks are typically bright green, aphyric to finely plagioclase-phyric pillow basalt and breccia. Calcite amygdaloidal pillows tend to be less than 0.5 m in long dimension and are commonly rimmed by bright red jasper, and/or occur with interpillow jasper (Figure 7). This unit is well exposed 7 km west-northwest of Newmont Lake where it is overlain by rubbly carbonate matrix to flow-top breccia fragments contains abundant large crinoids ossicles (Figure 5) and grades into thick-bedded carbonate containing basalt scoria. The carbonate locally forms crinoidal packstone.

The lower contact of the mafic volcanic unit is poorly defined. In northeast part of the area, the mafic volcanic rocks overly polymictic conglomerate and are intercalated with Viséan felsic volcanic rocks.

Felsic volcanic rocks

Carboniferous felsic volcanic rocks comprise white, pink and pale green weathering and aphyric to quartz-



Figure 7. Irregular flow top on Carboniferous pillow basalt is infilled with carbonate containing abundant large fossil crinoid stems (*i.e.* few centimetres above fingers). Pillows are outlined, and in some cases veined, by red jasper. Flow-top breccias grades into well-bedded carbonate containing basalt scoria.

phyric tuff and rhyolitic to dacitic locally flow-banded effusive units. The upper part of the section is characterized by well bedded, decimetre-thick, normal-graded felsic ash flow tuff beds which may be underlain by coarse basal breccia (5-10 m) thick, and may grade upwards into thin cherty dust tuffs beds (Figure 8a). These units define separate eruptive cycles that preserve 2-300 m of felsic ejecta interbedded with the pillowed and hyaloclastite basalt (Figures 8b, c), particularly well-

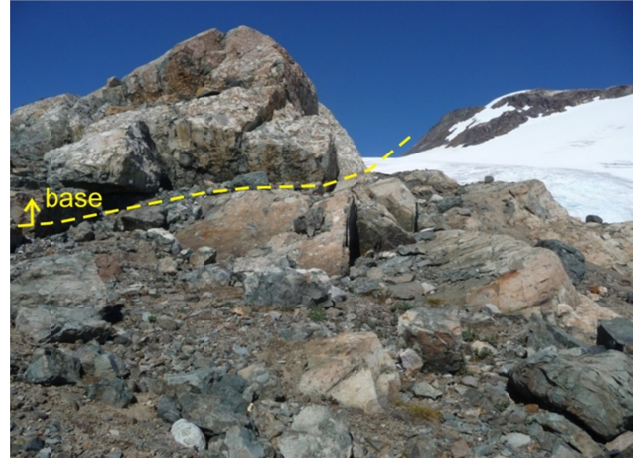


Figure 8a. Early Carboniferous felsic ash flow and block breccia. Contact line highlights the top of one eruptive unit and coarse base of the next.



Figure 8b. Early Carboniferous pillow breccia with hyaloclastite matrix.



Figure 8c. Early Carboniferous basaltic pillows and tubes.

displayed in the north and eastern portions of the map area. Pink weathering, quartz-phyric rhyolite dikes that commonly cut the section may be related to felsic volcanic rocks. Bedding tops suggest an upright facing volcanic section which projects beneath mid-Carboniferous (?) carbonate that is distinguished by the presence of large (>3.5 cm) crinoids ossicles. A preliminary isotopic age determination of ~340 Ma from a felsic tuff unit near the top of the succession confirms the Early Carboniferous (Viséan) age (N. Joyce, unpublished data).

Mid-Carboniferous carbonate

An approximately 190 m thick section of carbonate is dominated by thinly-bedded sets to massive metre-thick beds of crinoidal limestone (Figure 9a) with ossicles up to 4 cm diameter (Figure 5). Colonial coral heads more than a metre across are preserved. Bright green basalt clasts (Figure 9b), angular lapilli and reworked ash are of variable abundance, up to a maximum of ~15%. Volcanic content is sporadic, but generally decreases up section with pyroclastic debris all but absent more than ~40 m above the base of the unit. Planar chert beds are interlayered with crinoidal grainstone near the upper contact of the unit.

Coarse crinoidal packstone extends to the east where it has been extensively sampled for fossil age determination (Logan *et al.*, 2000). Faunas providing the most precise age control reveal a Serpukovian to Bashkirian age (~328-312 Ma), spanning the Lower Carboniferous (Mississippian) and Upper Carboniferous (Pennsylvanian) boundary.

Carboniferous chert-claystone

Parallel interbeds of grey to black chert and recessive light grey and yellow-weathering claystone form a distinctive unit above the Carboniferous carbonate. Chert beds 5 to 15 cm thick alternate (Figure 10) with recessive, poorly indurated claystone layers that are typically less than 5 cm thick. Rounded cloudy quartz grains ≤ 1 mm



Figure 9a. View to the north of a set of thin tuffaceous packstone beds flanked by more massive beds, each 1-1.5 m thick.



Figure 9b. Thickly bedded conglomeratic crinoidal packstone with scoraceous basalt clasts.



Figure 10. Very well bedded chert-siltstone-claystone unit contains distinctive grey and yellow weathering, recessive clay beds.

diameter within chert are interpreted as recrystallized radiolaria; although some white grains appear to have a cleavage and are likely reworked feldspar. Thus, the unit may be a distal turbidite and not strictly a biogenic pelagic ribbon chert succession.

Only a few exposures of this unit have been observed. It presumably grades into the underlying chert-bearing portions of Carboniferous carbonate, but a section that has not been structurally disrupted was not identified during the course of our mapping. Stratigraphic contacts with units of assumed Permian age are similarly disrupted or not exposed. Where best exposed, the unit is strongly deformed such that all that can be stated of the unit thickness is that it is more than ~10 m and probably less than 100 m.

Late Carboniferous (?)

Thickness of Upper Carboniferous mafic and felsic volcanic stratigraphy have been estimated as >1500 m north of the Scud River (Brown *et al.*, 1991; see their Figures 2-4) and in the Mess Creek area (Logan *et al.*, 2000) and are anticipated to crop out in the study area.

Varicoloured wacke, polyolithic volcanic conglomerate and fine grained turbiditic sediments at least 900 m thick that underlie the northeast corner of the Hoodoo Mountain area might belong to this unit. However, we interpret them as belonging to the Late Triassic succession (see following). Arguments for an Upper Carboniferous assignment can be made along strike to the north and we cannot unequivocally rule out such arguments. For example: these rocks occupy a structural, as well as upright facing position above mid-Carboniferous limestone and further northwest, apparently dip beneath Early Permian limestone as shown by Logan and Koyanagi (1994). The maroon to dark green conglomerate locally contains limestone cobble-rich layers and large (10 m²) olistoliths of Carboniferous limestone. Along strike to the north, the unit grades upward into maroon plagioclase phytic tuff which appears to conformably underlie limestone containing Late Carboniferous or Early Permian, Moscovian or younger corals and late Asselian to Sakmarian fusulinacean foraminifers, suggesting a conformable volcanoclastic sequence of probable Upper Carboniferous age.

Similar contact and faunal relationships have not been corroborated in the present study area where the varicoloured volcanoclastic section is interpreted to represent Upper Triassic deposition and cannibalism of older arc strata. Limestone granule conglomerate was collected for extraction of conodonts. If present, they will provide a maximum age for this unit.

Permian

Permian sections are comprised of massive to well-bedded carbonate and lesser chert. In most sections there is little or no evidence of volcanic debris. Although they are very diverse in detail, three mappable Permian units are separated herein: massive light grey carbonate, dark grey chert-carbonate, well bedded grey and cream carbonate. All of these units are correlative with the Permian Ambition Formation ~50 km to the north (Gunning *et al.*, 1994), where its thickness ranges between 500 and ~1100 m.

Well bedded grey and cream carbonate

Medium grey to cream-coloured carbonate is typically well bedded and fossiliferous. Large rugose corals, fenestrate and branching bryozoa, brachiopods, gastropods and giant fusulinaceans are common. Fossil debris may dominate some layers (Figure 6 and Figure 11) forming packstones. An Early to Middle Permian age is proposed for this unit on the basis of fossil age determinations from units along strike (Logan and Koyanagi, 1994; Brown *et al.*, 1996), where they range from Latest Carboniferous (Gzhelian) through Early Permian to Middle Permian (Roadian and Wordian). This is supported by the occurrence of giant fusulinaceans which are typically of Rhodian to Wordian age. (Brown *et al.*, 1996 and Logan *et al.*, 2000 used the Harland *et al.*, 1990 time scale which lacked a Middle Permian. As a



Figure 11. Bryozoan packstone within Early to Middle Permian section. Silicified branching and fenestrate bryozoan fossils form layers up to 30 cm thick.

consequence, they considered Roadian to be an Early Permian stage; both Roadian and Wordian stages are now included in the Middle Permian (Okulitch, 1999; Ogg *et al.*, 2008)).

Dark grey chert and carbonate

Irregularly bedded dark grey chert and carbonate tends to be relatively impoverished in macrofossils. Bulbous to hackly, chert layers and nodules up to 30 cm thick are crudely stratiform and are generally less than half the thickness of adjacent micritic carbonate layers, which may be fetid. Chert is presumably secondary as sponge spicules that could provide a source of silica could not be identified in outcrop. This unit appears to be in abrupt contact with overlying massive carbonate.

Massive light grey carbonate

Medium to coarse crinoidal grainstone commonly forms massive, light grey outcrops that lack any obvious bedding. Most outcrops contain at least sparse horn coral fragments and they may be abundant in some layers, typically best preserved where replaced by silica. Fossil horn corals may exceed 10 cm diameter and 30 cm in length. Unlike Carboniferous carbonate, crinoid ossicles are generally less than 0.5 cm diameter (not several centimetres). In two localities near the eastern edge of the map area, this unit is overlain by strata interpreted as Middle to Late Triassic age.

Early to Middle Triassic

Strata interpreted to be of Early to Middle Triassic age comprise a condensed section of graphitic cherty argillite with thin, fetid limestone and wacke layers. This sediment-starved package displays a fault-modified contact with underlying massive Permian carbonate, elsewhere it may be entirely removed by subsequent Late Triassic erosion.

Triassic cherty argillite

Black and rust, well bedded volcanic chert and sooty argillite comprises a section that is rarely exposed, and has not been observed undeformed. The deformed section is estimated to have a true thickness of less than ~40 m (Figure 12). It is composed of 3-6 cm thick cherty volcanic layers with generally thinner sooty argillite interbeds. Cherty layers are comprised of a significant proportion (up to ~10%) of silt and sand-sized lithic grains that could be water lain tuff, although an immature volcanic silt/sand source cannot be ruled out.

Laminated carbonate

Light grey to black, poorly indurated marl occurs as well laminated layers up to 20 cm thick within the chert-argillite-dominated section. At one locality, at least two of the marl layers are packstones of paper-thin bivalves tentatively identified as *Daonella* or *Halobia* of Middle to Late Triassic age. Subequal hinge-parallel and -normal dimensions favour the latter identification. Unfortunately bedding-perpendicular cleavage typically results in slabby weathering and incomplete fossil preservation.

Late Triassic

Late Triassic strata are dominated by volcanoclastic units, particularly polymictic boulder conglomerate. Distinctive coarse biotite- and K-feldspar-bearing conglomerate occurs together with hypabyssal rocks from which they were derived. Augite-phyric flows, a hallmark

of the Stuhini Group, are present, but are less abundant than clastic rocks. The conglomerate is variable, green, purple or maroon; dominantly matrix-supported in a poorly sorted chaotic groundmass of plagioclase and pyroxene crystal and lithic sand-sized grains. Horizons are often characterized by clasts of sedimentary units, particularly recrystallized and/or fossiliferous limestone. An interval of dacite ash-flow occurs near the top of the clastic section yields a preliminary U-Pb zircon age of ~220 Ma.

Turbiditic arkosic sediments

Well bedded turbiditic sediments are comprised mainly of graded volcanic sandstone- argillite couplets, but also include conglomerate. Blocky, cliff-forming outcrops of this unit weather olive brown. Graded turbidite couplets are typically 1 to 15 cm thick (Figure 13a). Basal scours and local development of ripple cross-stratification near bedding tops are features consistent with deposition from turbidity currents. Conglomerate beds contain subangular to rounded cobbles to small boulders of medium grained augite-porphyry (25% pyroxene and 20-25% fine to medium-grained plagioclase) and angular intraformational rip-up clasts (Figure 13b).

This unit rests unconformably on basinal strata of presumed Middle Triassic age. Olistostromal blocks metres across have been derived from the underlying chert and sooty argillite.



Figure 12. View to the north of rusty black chert, argillite and grey carbonate of interpreted Early to Late Triassic (?) age (fossil age determinations are pending). Blocky olive-brown rocks in the upper third of the section are conglomeratic volcanic wacke of presumed Late Triassic age. To the immediate east, the unit is underlain by massive grey limestone of presumed Permian age.



Figure 13a. Typical Late Triassic turbiditic sandstone-argillite couplets.



Figure 13b. Angular to rounded augite porphyry boulders and angular intraformational rip-up clasts.

Augite-phyric volcanic and epiclastic rocks

An apparently continuous section more than ~340m thick of coarse, crowded augite-phyric flows and breccia is exposed on nunataks north of Twin Glacier. Rocks of similar character extend to the west, outside of the mapped area, and could represent a section more than 1000 m thick. This unit is light olive green to brown and is blocky weathering. Conspicuous, euhedral, often zoned pyroxene comprises 15-30% of flows and breccia. Pillows are locally well developed with light grey and siliceous intrapillow laminated sediment. Vesicles commonly comprise a few per cent by volume and are infilled with calcite and sparse chalcidony. Well bedded maroon tuff layers up to several metres thick are interlayered with the flows.

Feldspar-phyric breccia and epiclastic rocks

Green to grey weathering, feldspar-phyric breccia and associated epiclastic rocks are extensively exposed in two areas: Upper Twin Glacier in east-central 104B/14E, and on south and east flanks of Verrett Mountain. Angular, coarse breccia, without significant epiclastic

components, is particularly well displayed in the upper Twin Glacier area where it is associated with pillowed, augite- porphyritic basalt. Typical lithologies contain medium grained, tabular feldspar that may display trachytic alignment and comprise 5-35% of the rock. However, grain size ranges from fine to coarse and pyroxene commonly accompanies feldspar. Quartz, carbonate and chlorite-filled vesicles can comprise up to 5%, or rarely 15%, of the unit. Chlorite, carbonate and epidote alteration and veining is common. Clasts, which could have been derived from this or similar units, comprise the dominant clast type within the dark brown and orange-weathering conglomerate and parts of the polymictic conglomerate unit.

Polymictic boulder conglomerate

The most widespread unit of the Stuhini Group in 104B/14E is a conspicuous polymictic boulder conglomerate. It crops out in a northwest-trending belt across the northern half of the map area where it probably attains a thickness of at least 2000 m. It is maroon to brown weathering and forms rounded outcrops and cliffs in which boulders of contrasting lithology are beautifully highlighted. Conglomerates belonging to this unit may be clast-supported, but are more commonly supported by a matrix of maroon ash tuffite or tuffaceous wacke. In order of decreasing relative abundance, common clast types include: medium to fine grained tabular feldspar-phyric volcanic tuff, coarse to medium grained augite and augite-feldspar porphyry, fine grained to aphanitic green to brown basalt, grey to white limestone (commonly fossiliferous and of presumed Paleozoic age), hornblende quartz diorite, recycled conglomerate, coarsely bladed plagioclase \pm K-feldspar porphyry, turbiditic wacke, pink medium- to coarse grained holocrystalline granodiorite, and in upper parts of the unit, dacite and picrite. The latter two clast types are recognized above a layer of ~220 Ma dacite tuff (Figure 14a).

Maroon tuff

Maroon to green water-lain tuff forms sections up to 200 m thick in the northeastern map area (along strike with Carboniferous strata PnSt, uCScg and uCSt on Logan and Koyanagi map) where it grades upwards into well indurated, coarse volcanic sandstone and then turbidites and carbonate-rich conglomerate with gastropods, crinoids and bivalves. Well bedded maroon, aphanitic to fine grained, lapilli and ash tuff to plagioclase tuffites occur close to the top of the section and these locally contain accretionary lapilli horizons. Planar, well-developed beds are typical.

Lithologies typical of this unit also occur as distinctive layers within several other units such as augite porphyry flows, turbidite and polymictic conglomerate within both Paleozoic and Mesozoic sections (see especially “Late Carboniferous (?)” above).

Dacitic ash flow

Crowded tabular feldspar and quartz-phyric dacite ash tuff comprise two layers near the top of the polymictic boulder conglomerate unit (Figure 14a). The thickest, upper layer attains a thickness of between ~80 m and ~130 m. It is a maroon and pinkish to grey and blocky weathering, resistant unit. Medium grained tabular plagioclase and lesser, coarser K-feldspar together comprise 35-40% of the unit with quartz eyes up to 0.5 cm diameter (Figure 14b) comprising ~5%, with lesser altered biotite (~3%) and sparse titanite. Some crystal-rich, flattened fragments may have been pumiceous and compacted during partial welding in an ash flow. Flow banding is conspicuous in some fragments. The uppermost 1-3 m of the unit is a tan weathering and slightly recessive probable airfall and reworked lithic lapilli crystal ash tuff. A preliminary isotopic age determination from a sample of this unit has returned a Late Triassic, ~220 Ma age (N. Joyce, unpublished).

K-feldspar megacrystic tuff, breccia and hypabyssal rocks

Texturally diverse tuffaceous, fragmental and hypabyssal rocks containing fragments of syenite and K-feldspar megacrysts are intermittently exposed over a broad region within east-central 104B/14E. This unit is characterized by abundant detrital biotite, comprising up to 25% of the rock.

Locally, the K-feldspar porphyritic and biotite rich fragmental rocks clearly exist as clastic dikes. Where such dikes cut contemporaneous strata, the distinction between intrusive, extrusive and immature epiclastic modes of occurrence is less obvious (Figure 15a). Hypabyssal units locally display delicate glomeroporphyritic K-feldspar “flowers” which are unlikely to have been preserved in an ash cloud or sedimentary environment. Some bombs of trachytic, crowded K-feldspar porphyry display a mantle of vesicular glass (*i.e.* chilled; Figure 15b). This same crowded K-feldspar porphyry comprises one of the several slight variants of K-feldspar megacrystic dikes in west-trending swarms, some of which display porphyry-style copper mineralization (see later section: “Intrusive Rocks”).

Late Triassic to Early Jurassic

Dark brown and orange-weathering conglomerate, wacke and coal

Dark brown conglomerate is dominated by well-rounded, finely tabular feldspar-phyric clasts and conspicuous pink-orange syenite and coarse K-feldspar crystals derived from the unit described previously. In most places the unit is carbonate-altered and weathers orange. Clasts are typically supported by a distinctive matrix of immature sandstone containing as much as 5% detrital biotite up to 1.5 cm diameter. Locally the conglomerate passes laterally or vertically into well-bedded wacke (Figure 16a) and in places is tuffaceous

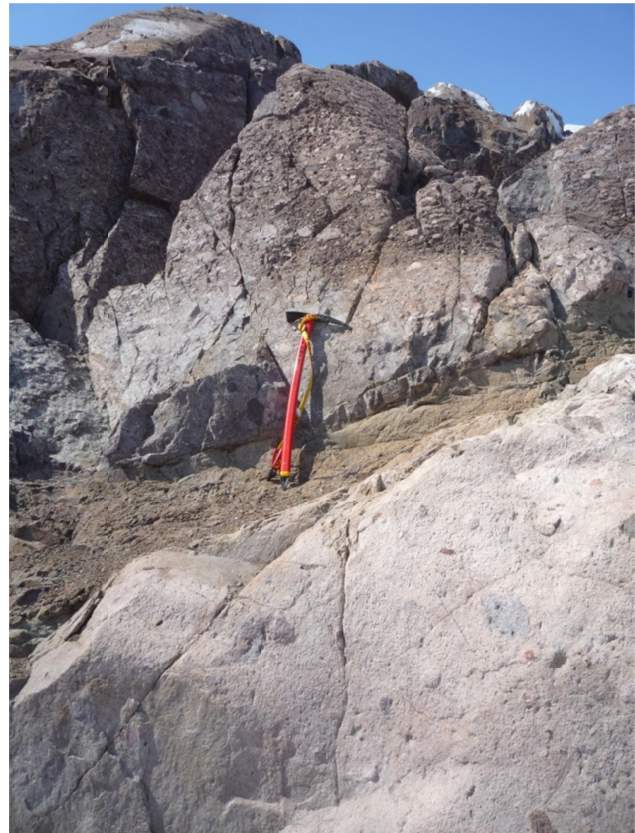


Figure 14a. Polymictic conglomerate (above ice axe) overlies light pink lithic lapilli crystal ash tuff (marking top of ash flow cooling unit). An unconformable contact is marked by a layer of tan weathering reworked tuff (at base of ice axe).



Figure 14b. Close-up of quartz-phyric dacite ash tuff.

with pink lapilli that include megacrystic K-feldspar crystals. Wacke layers commonly contain coaly plant fragments. One distinctive fossilized plant includes an



Figure 15a. Angular pink syenite fragments as well as K-feldspar crystals float within an orange-weathering matrix. Silvery glints are altered biotite crystals. Multiple generations of erosion or brecciation and milling have produced clasts of clastic material. Planar, dike-like bodies of the same clastic material (top and right side) appear to have cut the rock body.



Figure 15b. Boulder sized, trachytic, crowded K-feldspar porphyry clast, perhaps a bomb (?), is mantled by glassy vesicular material.

artichoke-like cone/flower with nested woody scales/petals, perhaps *Williamsonia*, a cycad common in the Jurassic (Figure 16b; extraction and identification of fossil pollen from a collected sample is pending).



Figure 16a. Orange-weathering conglomerate interbedded with graded arkosic sand and siltstone.



Figure 16b. Within coal-rich parts of the unit, wood fragments are common (bottom edge of photo) as are scales of an artichoke-like fossil (arrows).

Hornblende-feldspar ash flow and breccia

Resistant, blocky to rounded weathering, hornblende ± biotite dacite ash flow forms a distinctive unit about 100m thick. It is medium grained and light grey to light maroon or green where chlorite- and epidote-altered. Partly welded ash flow and flow top breccia textures are well displayed. Acicular, euhedral oxyhornblende comprise 5-10% of the unit and tabular feldspar commonly comprises 35-40% (Figure 17). Ash flow is in sharp contact with deep maroon ash tuff which may have been part of the same eruptive event. Brecciated zones may have a carbonate matrix and eruptive units are interbedded with limestone matrix-supported conglomerate beds typically less than a metre thick.

Preliminary age determination on a sample of hornblende-plagioclase ash flow breccia yielded a ~187 Ma age (N. Joyce, unpublished data) confirming Early Jurassic magmatism in the Hoodoo Mountain area. Britton *et al.* (1990) note that these Dacitic rocks are texturally similar to the “Premier Porphyry” unit that marks the top of the Unuk River Formation and base of the Betty Creek Formation. Representative isotopic age



Figure 17. Chlorite-altered hornblende ±biotite and feldspar crystal ash flow tuff.

determinations from the Betty Creek Formation are: $187.7^{+5.8}_{-1.5}$ Ma and $187.7^{+5.3}_{-4.4}$ Ma (U-Pb, abraded zircons; Lewis, 2001).

Hoodoo tuff

The youngest volcanic rocks identified within the eastern Hoodoo Mountain area are flows, un-lithified soil and wind-sorted scoria of the *ca.* 28 to 1800 Ka Hoodoo Mountain volcanic complex (Figure 18; Edwards *et al.*, 2000). Flows which have emanated from the extinct Hoodoo Mountain volcano are exceptionally well exposed near the toe of western Twin Glacier where they unconformably overly polydeformed rocks. Tan to brown aphanitic and scoriaceous lapilli and ash occupy hollows in the high ridges in the western part of the area and form relicts of a presumably once continuous blanket where it has not been removed by rain, wind or ice. Mapping the lower elevation extent of these relicts could provide limits for glacier extents at the time of eruption; however, our work did not include such mapping, as we have focused on rock packages of importance for mineral exploration.

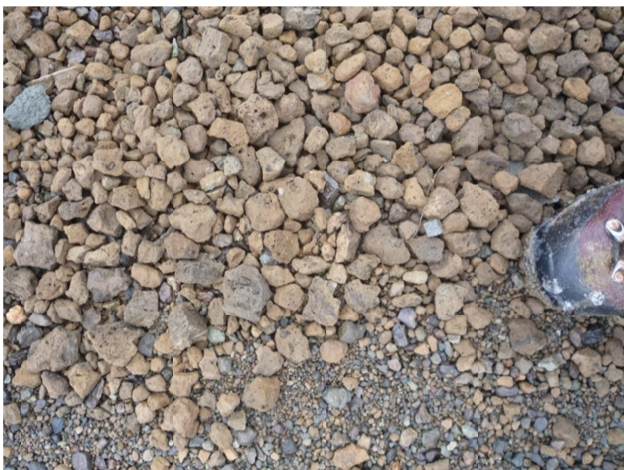


Figure 18. Lapilli sized, pumiceous scoria, probably originating from the extinct Hoodoo Mountain volcano. These deposits and derived soils cap many of the ridges in western 104B/14E and restrict glacial ice extents at the time of eruption to an elevation of less than ~1240 m (less than 240 m above its current level).

Preliminary $^{40}\text{Ar}/^{39}\text{Ar}$ age determinations from volcanic samples collected at Hoodoo Mountain are reported by Edwards *et al.* (2000) as ranging from 28 to 1800 Ka (no error limits on personal communication from M. Villeneuve, 1998).

INTRUSIVE ROCKS

Three main intrusive units and several suites of dikes cut stratigraphy within the Hoodoo Mountain area. Of these, deformed granite exposed in the upper Verrett River valley and an undeformed pluton extending from the Verrett River to Twin River, are by far the most voluminous (Figure 3).

Verrett pluton - graphic granite

Graphic granite is exposed in the upper Verrett River valley. We follow the nomenclature of Logan *et al.* (2000) who called it the Verrett Pluton. Within the eastern Hoodoo Mountain map area, the Verrett pluton is white to tan and rust weathering, forming blocky to low, rounded outcrops. It is composed mainly of subequal amounts of intergrown quartz and K-feldspar (Figure 19). Feldspar is turbid due to alteration to white mica and carbonate. Anhedral pyrite grains locally comprise up to 3% of the rock. In places the body appears clastic, due to structural cataclasis. Contacts with adjacent units are both faulted and intrusive. Its northern contact crosscuts Carboniferous volcanic and sedimentary bedding at high angle and locally displays a narrow chilled margin adjacent to country rock. Verrett pluton was tentatively correlated with the Late Devonian Forrest Kerr plutonic suite (Logan *et al.*, 2000). It is undated, but if it intrudes Carboniferous volcanic rocks, as it appears to in the Hoodoo map area (Figure 3), it cannot be Devonian in age. If these contact relations are correctly interpreted, the Verrett Pluton must be at least as young as Carboniferous. An isotopic age determination from a sample of this unit is pending.

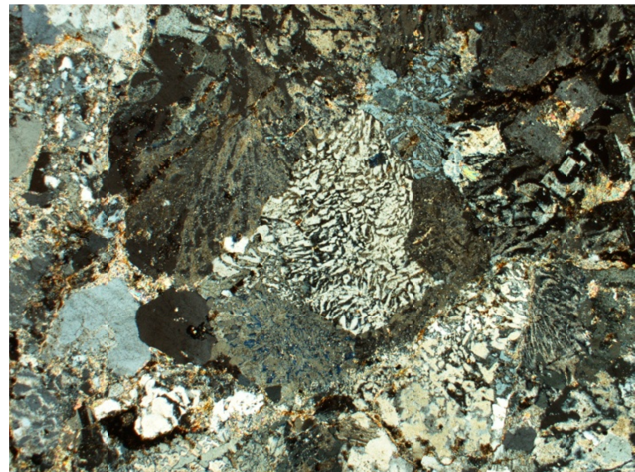


Figure 19. Verrett pluton graphic granite of interpreted Devonian age. Note clastic texture along left margin in this cross polarized light 4 mm field of view.

Biotite-rich diatreme

Dark grey-brown weathering dike-like bodies of clast- ±xenocryst-rich biotite syenite (Figures 20a, b, c) cut across Mesozoic and Paleozoic strata within central and eastern 104B/14E. Where weathered, rounded clasts may be plucked from rubbly debris, but fresh outcrops are blocky, highly compact, and difficult to break. Phenocrysts include: biotite ~25%, diopsidic (?) pyroxene 5%, K-feldspar 5% with minor aegirine and accessory apatite and opaque grains. Matrix mineralogy is 40% K-feldspar (±feldspathoids (?)) and up to 20% carbonate occurring as patches. Biotite occurs as three distinct modes: oldest are coarse grained dark brown to black pleochroic crystals altered by carbonate and having expanded basal plates with abundant opaque inclusions, second are medium grained, golden to green-tan pleochroic elongate and ragged crystals that are commonly kinked or warped, youngest are fine- to medium grained, zoned, dark brown to dark green pleochroic crystals that commonly occur as clusters of euhedral booklets. Pyroxene is bright green and occurs glomerocrysts, euhedral crystals and crystal fragments. Outsized, bright green pyroxene crystals are interpreted



Figure 20a. Dense and compact biotite syenite containing a large xenocryst of bright green pyroxene, probably chrome diopside.



Figure 20b. Where weathered, milled clasts fall from the intrusive matrix.

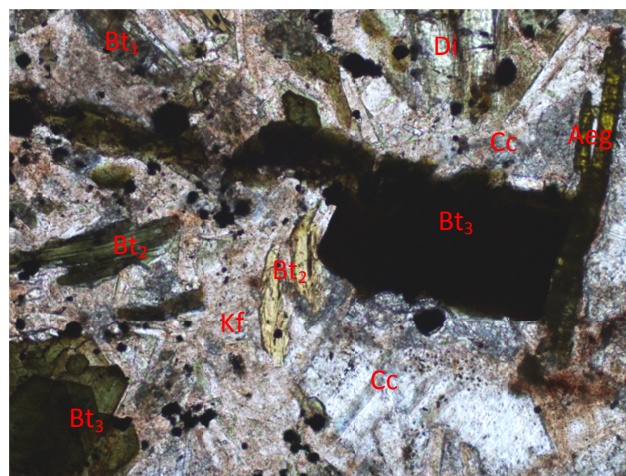


Figure 20c. Photomicrograph showing multiple generations of biotite ($Bt_{1,2,3}$), a matrix of K-feldspar (Kf) and carbonate (Cc), a phenocryst of aegirine (Aeg), and a xenocryst (?) fragment of diopside (Di). Plane polarized light view of ~2 mm field of view of sample MMI10-18-9.

as chrome diopside xenocrysts; although no evidence of crystal disequilibrium is seen in thin section. Positive identification awaits microanalytical investigation. K-feldspar phenocrysts range up to 1.5 cm and may form Carlsbad twins or glomerocrysts. Xenoliths are dominantly pink syenite and may be highly spherical indicating significant milling during diatreme emplacement.

Biotite-rich diatreme dikes are commonly spatially associated with K-feldspar megacrystic dikes or breccia dikes. These dikes probably occupied vents feeding pyroclastic eruptions as evidenced by the extrusive tuffaceous equivalents found in the K-feldspar megacrystic tuff and related rocks.

Mesozoic to Tertiary varitextured melano-granodiorite

Light to dark grey, blocky weathering hornblende melano-granodiorite forms an irregularly-shaped body that extends north from the southeast flank of Mount Verrett. Hornblende and plagioclase are randomly intergrown forming fine grained to pegmatitic zones or alternating hornblende and quartz-feldspar-rich layers (Figures 21a, b). Feldspar may be altered to white mica, and both hornblende and subordinate biotite are chlorite-altered. Fine miarolitic cavities may be lined with feldspar and quartz and infilled with chlorite. Secondary calcite commonly occurs near the margins of accessory titanite.

No age has been determined for the varitextured melano-granodiorite; however, it conforms to the eastern margin of the Twin River pluton and may be an earlier phase of the pluton which has been intruded by more leucocratic granodiorite. Previous maps show the Twin River pluton as Eocene in age. Youngest rocks cut by the melano-granodiorite are interpreted to be of Late Triassic age. A persistent set of several metre thick dikes is lithologically similar and cuts strata that may be as young as Early Jurassic.



Figure 21a. Textural variability in hornblende granodiorite: pegmatitic zone with intergrowths of K-feldspar plagioclase and hornblende within texturally diverse melano-granodiorite.



Figure 21b. Textural variability in hornblende granodiorite: compositional banding and including pegmatitic zones.

Eocene Twin River granodiorite

Light grey to white weathering, blocky, hornblende-biotite granodiorite forms a 50 km², northwest-elongated pluton; the largest in the map area. Herein called the Twin River pluton, it extends from Mount Verrett to Twin River. A compositionally similar, satellite stock is exposed 15 km farther to the northwest.

The most abundant phase is a medium grained, salt and pepper granodiorite that contains black and vitreous hornblende (5-10%, some with biotite in cores) and sub-euhedral biotite booklets (10-15%). Plagioclase is oscillatory reverse zoned with an average anorthite content of ~An₂₇₋₃₀. Composition of the body tends to be uniform with the exception of contorted hornblende-rich screens and contact zones, especially with melano-granodiorite, which may be xenoliths-rich (Figure 21c). Thermal metamorphism attributed to the Twin River pluton extends for several hundred metres from its mapped contacts. Schistose rocks south of the pluton are mineralized with chalcopyrite and possibly traces of native gold.



Figure 21c. Textural variability in hornblende granodiorite: contact zone with Twin River granodiorite (light matrix) is rich in xenoliths of hornblende granodiorite.

ECONOMIC GEOLOGY

Previous Exploration

Mineral claims were first recorded for the Iskut River area in the early 1900s followed shortly thereafter by a one ton shipment of Johnny Mountain ore that yielded 2.05 grams gold, 1.37 kilograms silver and 12.45% copper (Clothier, 1918). Subsequent exploration work focussing primarily south of the Iskut River began with discoveries of high grade auriferous massive sulphide mineralized float in 1954 by Hudson Bay Mining & Smelting Ltd. (Pickaxe). In 1969, R. Gifford restaked and vended the Inel property to Skyline Exploration Limited (Gifford, 1980) who explored and developed the Inel and Reg/Stonehouse properties. From 1988-90 and 1993, the Johnny Mountain Mine produced 4.34 million grams of silver, 2.81 million grams of gold and 1 008 000 kilograms of copper from steep dilatational quartz-pyrite veins at the Stonehouse deposit from 225 247 tonnes milled before shutting down due to low metal prices (BC MINFILE, 2010). At about the same time, Delaware Resources Corp. and Cominco Ltd. had delineated approximately a million tonnes of 27 g/t Au on the Snip property, about 5 km north of the Johnny Mountain Mine. Between 1991 and 1999, the Snip deposit produced 32.093 million grams of gold, 12.183 million grams of silver and 249 276 kilograms of copper from from about 1.2 million tonnes of ore (BC MINFILE, 2010).

North of the Iskut River, a major exploration and geological mapping program was undertaken by Newmont Mining Corporation of Canada Ltd. (Newmont) in 1972. It was the era of copper porphyry exploration, and in this region efforts were directed towards copper-iron skarn mineralization associated with feldspar megacrystic syenite intrusions on the Dirk and Ken showings. Gulf International Minerals staked the McLymont claims south of Newmont Lake in 1986 to cover auriferous skarn mineralization. Recent work covering the Dirk and Newmont Lake areas has been

conducted by Romios Gold Resources (Ray, 2006; Bernales *et al.*, 2008; Chadwick and Close, 2009).

Late Triassic Copper Mountain Intrusive-Related

Copper, gold and silver mineralization at the Dirk, Telena and Birthday Jim prospects is related to a regionally extensive Latest Triassic alkaline magmatic event, the Copper Mountain Plutonic Suite (Woodsworth *et al.*, 1992). This magmatic event is causative to porphyry mineralization along the length of British Columbia. In the northwest, related mineralization is found at Galore Creek, Red Chris and GJ. In central and southern BC, related deposits include Mount Polley, Afton and Copper Mountain.

Dirk Showing (MINFILE 104B 114)

In 1972, Newmont carried out geological mapping, airborne and ground magnetometer surveys and drilled six holes totalling 93.87 m. Three holes were drilled at each of the Dirk and Ken claims using a Winkie drill and "A" drill string (the Ken zone is located 5.5 km east of the Dirk on NTS map sheet 104B/15, east of the study area that we report on here). It was concluded then that the Winkie drill was an ineffective tool for sampling these zones (Costin, 1973). In 2009, Romios Gold Resources conducted followed up geological investigations (Chadwick and Close, 2009) and sampling of the mineralization on two of the known mineral showings: the Dirk and Telena zones, which are separated by a kilometre-wide expanse of glacier.

The Dirk prospect occupies the eastern margin of an alkaline intrusive center more than 3 by 4 km in size. The intrusive centre is a swarm of easterly-trending sills and dikes as well as stock-like bodies of texturally variable, porphyritic and equigranular syenite containing orthoclase \pm pseudoleucite. K-feldspar porphyry bodies are identical to the Late Triassic "rhomb porphyries" of the alkaline feldspar porphyry intrusive suites at Galore Creek, located 40 km to the northwest. Crystallization ages of the intrusions at Galore Creek range from 210.2 \pm 1.0 Ma (U/Pb, titanite; Mortensen *et al.*, 1995) for a syn-mineral dike to 208.8 \pm 0.8 Ma (U/Pb, zircon; Logan, unpublished) for a post-mineral dike. The Dirk intrusions, like those at Galore, are silica-under saturated, syenite and foid-bearing syenite characterized by centimetre-scale megacrysts of orthoclase and smaller phenocrysts of biotite, sodic pyroxene, hornblende, apatite, magnetite, and titanite. They are variably altered, containing assemblages of andradite garnet, epidote, clinozoisite, secondary biotite, chlorite, calcite and anhydrite (?). Diatreme bodies containing breccia fragments of distinctive porphyritic syenite and bright green pyroxene form part of this magmatic suite and are cut by younger syenite dikes containing coarse orthoclase crystals.

The main Dirk showing is an east trending eight metre wide skarn zone of patchy bornite, covellite and

chalcopyrite \pm pyrite mineralization replacing limestone adjacent to pink, potassium feldspar-phyric syenite dikes. Sulphides occupy millimetres thick veinlets and irregular patches locally with magnetite and/or andradite, epidote and albitic (?) alteration. Metal assemblages of economic interest include chalcopyrite \pm gold. Alteration assemblages (*i.e.* magnetite, specular hematite, andradite and epidote) infer a highly oxidizing character of the main hydrothermal event. Late stage iron carbonate and barite veins are common at the Dirk and Telena zones. Eight, 1 m chip samples taken along a north-south traverse across the main Dirk showing returned 2.9% Cu and 0.64 g/t Au (Chadwick and Close, 2009). Additional copper-gold mineralization has been recognized 200 m southeast of the main zone and a 3.0 m chip sample from this mineralized section assayed 6.21% Cu and 0.57 g/t Au (Chadwick and Close, 2009). A sample collected during the course of our mapping contained >1% Cu, 5 ppm Ag, 0.6 ppm Au and 0.38% Zn (see sample 10JLO-254, Tables 1 and 2).

Telena Showing

Mineralization at the Telena showing is described as a 40 by 40 m cliff exposure of disseminated and vein chalcopyrite with intermittent bornite-bearing breccias within a syenite porphyry (Chadwick and Close, 2009). A reported grab sample from the Telena Zone assayed 2.07% Cu and 0.97 g/t Au. Two samples were collected during the course of our mapping. These are representative of the two ends of the spectrum of mineralized K-feldspar porphyritic rocks. One sample was collected from largest of many irregular patches and veins of semi-massive chalcopyrite (~0.25 by 1.1 m) within a strongly copper-stained, brecciated and skarnified coarse K-feldspar and calcite amygdaloidal porphyry. A second sample was collected from a relatively poorly mineralized dike at least 4 m thick, which cuts across the unit from which the first sample was collected. This dike contains medium to coarse K-feldspar phenocrysts. Notable results from analysis of these two samples are: Cu, >10 000 ppm, 1058 ppm; Au, 4.1 ppm, 0.1 ppm; Ag, 15.5 ppm, 0.7 ppm; Pd, 64 ppb, 27 ppb; Pt, 21 ppb, 3 ppb (samples MMI10-18-11 and MMI10-18-11b, Table 1).

About 650 m southwest of the Telena is a 2 km long, west-trending nunatak. It largely underlain by an east-northeast striking dike swarm of calc-potassic altered megacrystic potassium feldspar syenite dikes which abut against and intrude a large olistostromal block of thick bedded recrystallized limestone forming the eastern end of the nunatak. Brecciated, white orthoclase flooded syenite porphyries overprinted and replaced by brown or green euhedral zoned andradite garnet, anhydrite, traces of malachite and late carbonate attest to a vigorous magmatic/hydrothermal centre.

Table 1. Selected elements from Inductively Coupled Mass Spectrographic analyses (ICPMS) of samples collected in the Hoodoo Mountain area. For entire dataset see Mihalynuk *et al.* (2011b).

Sample Number	Latitude	Longitude	Lab Number	Ag	As	Au	Ba	Bi	Cd	Ce	Co	Cs	Cu	Fe	Ga	Hg	K	Mn	Mo	Pb	Pd	Pt	S	Se	Te	Th	Y	Zn	Zr		
			Detection Limit	PPB	PPM	PPB	PPM	PPM	PPM	PPM	PPM	PPM	PPM	%	PPM	PPB	PPM	%	PPM	PPM	PPB	PPB	%	PPM	PPM	PPM	PPM	PPM	PPM		
10JLO-161	56.9093	-131.0831	62121	260	37.1	27.9	50.1	1.97	1.41	31.7	17.1	0.36	69.37	4.3	7.1	90	0.16	879	0.66	16.3	<10	4	2.75	1.6	0.18	2.6	10	203.4	2.2		
10JLO-161	56.9093	-131.0831	62121	276	36.6	24.7	50.2	2.05	1.38	31.5	17.1	0.4	69.59	4.38	7.1	70	0.15	894	0.61	17.28	<10	4	2.74	1.3	0.2	2.7	9.93	211.1	2.4		
10JLO-182	56.8819	-131.0340	62122	3839	23.2	6403.5	22.4	0.26	0.08	5.4	12.1	0.04	5163.48	6.63	4.8	171	<0.01	1698	2.05	1.89	<10	4	0.23	0.3	0.05	0.6	7.94	33.1	5.4		
10JLO-254	56.8713	-131.0280	62123	5049	208.7	625.3	11.5	0.48	10	2.9	602.5	0.11	>10000.00	23.36	3.9	29570	<0.01	2392	5.07	22.2	48	<2	0.04	2.3	0.26	0.2	2.02	3819.3	1.3		
10JLO-278	56.7071	-131.1140	62124	23534	85.3	2113.9	55.5	53.39	1.68	1.8	10	2.04	381.68	14.78	6.5	55	0.98	335	9.3	516.24	<10	<2	5.05	33.4	18.08	0.2	3.05	219	0.3		
MM10-1-05	58.7571	-133.7057	62125	16	0.6	7.4	27	0.03	0.12	0.4	20.5	0.09	8.09	3.83	7	<5	0.03	1523	0.12	3.32	<10	<2	0.08	<0.1	<0.02	<0.1	5.06	37.3	<0.1		
MM10-12-08	56.8210	-131.1433	62126	7497	11.1	1754.8	61.9	1.87	3.34	5.7	20.4	5.28	1567.05	6.9	12.9	54	2.45	1019	1.3	6.38	<10	<2	1.88	1.6	0.45	0.7	8.86	184.3	0.9		
MM10-12-12	56.8175	-131.1558	62127	101	4.3	6.6	151.4	0.08	0.07	16.5	9.5	1.44	38.5	3.29	2.1	12	0.2	1007	3.41	2.73	<10	<2	0.33	<0.1	<0.02	2.5	10.39	60.1	0.3		
MM10-13-07	56.8281	-131.1684	62128	24	5.3	2.8	17.3	<0.02	0.31	3.8	0.9	<0.02	23.57	0.36	3.6	30	0.01	548	0.12	5.13	<10	<2	0.03	<0.1	<0.02	0.5	1.84	6	6.3		
MM10-13-12	56.8321	-131.1570	62129	168	3.1	2.1	61.6	0.12	0.03	1.6	27.9	0.5	29.56	2.81	0.5	636	0.19	7	0.88	0.77	<10	<2	2.96	0.1	<0.02	1	1.32	3.5	5.4		
MM10-14-09	56.7473	-131.0294	62130	1039	3.1	6.7	111.2	0.28	0.05	8.2	12.3	3.07	233.65	3.26	7.7	14	0.63	92	1.01	6.53	10	2	1.95	0.7	0.26	0.5	1.95	17.8	1.1		
MM10-16-10	56.9797	-131.0662	62131	5843	<0.1	5	717.6	0.38	14.01	16.3	6.4	0.14	1616.02	1.8	4.8	1557	0.06	147	0.47	33.34	<10	<2	0.04	2.4	<0.02	0.3	7.12	4044.1	1.4		
MM10-16-10b	56.9797	-131.0662	62132	5970	0.3	4.6	742	0.37	14.47	16.6	6.5	0.14	1668.12	1.84	4.9	1564	0.06	146	0.43	33.03	21	<2	0.04	2.3	<0.02	0.3	7.53	4168.1	1.3		
MM10-16-10b	56.9797	-131.0662	62132	6223	<0.1	4.5	761	0.39	14.62	17.1	6.6	0.16	1719.17	1.91	5.3	1644	0.06	153	0.48	34.81	38	<2	0.04	2.3	<0.02	0.4	7.69	4297.5	1.5		
MM10-18-07	56.8811	-131.0332	62133	417	8.2	153.1	112	0.4	0.04	6.7	25.1	0.09	4474.48	8.03	0.7	1497	0.03	633	3.75	1.64	<10	<2	0.75	0.5	0.08	<0.1	5.4	9.3	1.1		
MM10-18-11	56.8604	-131.0384	62134	15522	208.4	4110.6	55.3	2.08	0.23	30.1	37.7	0.37	>10000.00	15.92	11.2	469	<0.01	2349	22.65	15.89	64	21	1.57	28.6	1.13	0.5	15.92	120.2	2.5		
MM10-18-11b	56.8604	-131.0384	62135	737	10.5	136.8	13.7	0.55	0.18	60.4	74.8	1.16	1068	7.18	4.2	92	0.05	3213	2.12	12.4	27	3	2.27	5.8	0.33	1.4	33.68	54	3		
MM10-20-12	56.8201	-131.0190	62136	1654	16.9	80.8	145.3	2.41	0.18	4.5	36.7	1.22	584.01	4.98	2.2	144	0.34	1631	4.14	5.14	<10	3	1.31	1	0.2	7.46	42.8	0.9			
MM10-20-12b	56.8201	-131.0190	62137	15657	63.2	736.6	30.8	49.5	0.22	2.5	37.8	0.37	2490.92	11.72	8.4	137	0.17	418	24.97	9.33	<10	<2	5.94	7.3	28.47	0.4	3.61	77.9	1.3		
MM10-20-13	56.8208	-131.0201	62138	441	23.7	<0.2	46.1	0.41	0.08	6.6	6.9	0.61	1064.39	2.39	0.7	20	0.19	1713	1.48	5.1	<10	<2	0.53	0.7	0.05	0.2	9.17	15.1	0.4		
MM10-22-06	56.8216	-131.0214	62139	100	3.2	2.4	124.3	0.06	0.04	2	7.3	0.16	311.75	2.86	0.4	8	0.09	387	1.5	1.21	<10	<2	0.59	0.2	0.02	<0.1	1.73	6.3	0.3		
MM10-24-03	56.7598	-131.1858	62140	260	6	6.7	46.2	0.07	0.07	2.9	17.4	1.22	249.87	2.25	3.7	18	0.29	393	0.83	9.72	<10	4	0.61	0.3	0.03	0.3	4.07	23.6	1.3		
MM10-24-04	56.7067	-131.1142	62141	3079	0.2	388.5	128.3	2.43	0.05	5.2	31.1	8.08	2000.94	7.13	13.1	<5	2.76	701	88.16	1.81	13	<2	1.78	4.6	1.48	0.5	3.87	74.3	0.4		
MM10-24-05	56.7070	-131.1141	62142	7139	22.8	885.2	78.5	15.65	0.23	6.2	10.7	4.59	4151.72	4.16	6.9	18	1.57	454	25.01	2.3	<10	2	2.22	7.7	5.96	1.3	9.11	43.5	0.5		
MM10-24-06	56.6785	-131.0937	62143	5495	197.9	584.6	32	31.81	0.28	5.1	21.3	2.57	1528.42	14.86	8.7	22	0.99	426	138.42	10.84	11	2	>10.00	35.4	7.4	0.5	5.89	41.1	0.9		
Reference Materials																															
Standard BCGS till			62144	1619	65.3	28.5	275.5	0.3	0.76	27.9	49.4	0.56	175.55	7.61	9.5	369	0.05	1604	0.92	236.26	<10	<2	<0.02	0.7	0.34	3.6	13.04	350.4	3.2		
Standard DS7			1020	51.7	87.6	425.2	5.1	6.41	39.9	9.6	6.59	103.9	2.41	4.8	219	0.46	634	22.28	74	83	39	0.21	3.3	1.39	5	6.23	393	5.9			
Blank				<2	<0.1	<0.2	<0.5	<0.02	<0.01	<0.1	<0.1	<0.02	<0.01	<0.01	<0.1	<5	<0.01	<1	<0.01	<0.01	<0.01	<10	<2	<0.02	<0.1	<0.02	<0.1	<0.01	<0.1		

Table 2. Selected elements from Instrumental Neutron Activation Analysis (INAA) of samples collected in the Hoodoo Mountain area. For entire dataset see Mihalyuk *et al.* (2011b).

Sample Number	Latitude	Longitude	Lab Number	Au	Ag	As	Ba	Ca	Co	Cr	Cs	Fe	Hf	Hg	Mo	Na	Ni	Rb	Sb	Sc	Se	Th	U	W	Zn	La	Ce	Nd	Sm	Eu	Tb	Yb	Lu	Mass	
			Detection Limit	ppb	ppm	ppm	ppm	%	ppm	ppm	ppm	%	ppm	ppm	ppm	ppm	ppm	ppm	ppm	ppm	ppm	ppm	ppm	ppm	ppm	ppm	ppm	ppm	ppm	ppm	ppm	ppm	ppm	g	
			Measure unit	5	5	2	100	1	5	10	2	0.02	1	1	5	0.05	50	30	0.2	0.1	5	0.5	0.5	4	50	1	3	5	0.1	0.2	0.5	0.2	0.05		
10JLO-161	56.9093	-131.0831	62121	<5	<5	42	2000	<1	14	50	<2	4.41	<1	<1	13	2.32	<50	140	2.7	11.3	<5	5.3	<0.5	<4	290	18	40	<5	2.5	<0.2	<0.5	1.5	0.32	35.2	
10JLO-182	56.8819	-131.0340	62122	6810	<5	35	700	12	14	70	<2	14.4	<1	<1	<5	0.05	<50	<30	2	5.8	<5	<0.5	<0.5	139	70	6	<3	<5	1	<0.2	<0.5	1	0.14	36.3	
10JLO-254	56.8713	-131.0280	62123	560	<5	238	500	<1	623	60	<2	51.5	<1	26	<5	<0.05	<50	<30	6.4	0.7	11	<0.5	<0.5	11	4520	4	<3	<5	0.3	<0.2	<0.5	<0.2	<0.05	45.2	
10JLO-278	56.7071	-131.1140	62124	1980	25	90	1200	2	10	220	4	13.2	2	2	<5	0.34	<50	<30	1.2	11.6	25	1.4	2.9	9	240	7	14	17	1.4	0.7	<0.5	1.4	0.29	45.2	
MM10-1-05	56.7571	-133.7057	62125	<5	<5	<2	<100	11	22	130	<2	4.75	<1	<1	<5	1.78	<50	<30	0.2	24.6	<5	<0.5	<0.5	<4	<50	1	8	<5	0.7	0.5	<0.5	2	0.3	33.1	
MM10-12-08	56.8210	-131.1433	62126	2400	9	18	1400	<1	22	40	6	7.01	2	<1	<5	1.96	<50	<30	9.8	18.6	<5	3.8	3	<4	<50	14	34	<5	3.3	<0.2	<0.5	2.7	0.41	34.5	
MM10-12-12	56.8175	-131.1558	62127	<5	<5	<2	400	4	10	50	<2	3.31	1	<1	<5	0.25	<50	50	1.5	13.6	<5	4.1	3.1	<4	80	12	25	14	2.3	0.7	<0.5	2.4	0.27	36.3	
MM10-13-07	56.8281	-131.1684	62128	<5	<5	32	300	11	<5	100	<2	2.12	1	<1	<5	0.16	<50	<30	3	7.7	<5	2.5	<0.5	<4	60	7	12	<5	1	0.4	<0.5	0.6	<0.05	42.3	
MM10-13-12	56.8321	-131.1570	62129	<5	<5	<2	2200	<1	28	100	3	3.75	2	<1	<5	0.27	<50	130	1.4	24.2	<5	2.9	5.9	<4	<50	6	12	16	1.1	<0.2	<0.5	3.1	0.5	26.9	
MM10-14-09	56.7473	-131.0294	62130	<5	<5	<2	4200	<1	11	80	7	3.26	6	<1	<5	0.28	<50	70	0.4	21.8	<5	4.6	<0.5	<4	<50	31	63	23	6.4	2.1	<0.5	5.3	0.82	35.1	
MM10-16-10	56.9797	-131.0662	62131	<5	7	<2	600	<1	8	120	<2	1.9	4	<1	<5	3.6	<50	<30	1.5	8.3	<5	2.4	2.5	<4	4040	9	17	<5	2.8	1	<0.5	4.4	0.67	34.7	
MM10-16-10b	56.9797	-131.0662	62132	<5	8	4	1200	3	8	140	<2	1.9	3	<1	<5	3.7	<50	<30	1.6	8.4	<5	2.4	<0.5	<4	4130	9	24	28	3.1	1	<0.5	4	0.67	32	
MM10-18-07	56.8811	-131.0332	62133	188	<5	20	<100	5	26	70	<2	29.4	<1	<1	15	<0.05	<50	<30	4.9	1.4	<5	<0.5	<0.5	91	<50	4	8	<5	0.8	<0.2	<0.5	0.7	<0.05	41.9	
MM10-18-11	56.8604	-131.0384	62134	4260	17	200	<100	6	366	40	<2	14.8	<1	<1	22	<0.05	230	<30	9.1	14.4	27	<0.5	<0.5	21	150	23	29	25	2.8	0.9	<0.5	3.8	0.64	37	
MM10-18-11b	56.8604	-131.0384	62135	135	<5	15	<100	20	73	30	<2	12.2	<1	<1	<5	<0.05	<50	<30	5.9	14.2	<5	1.1	3.1	10	<50	48	61	<5	4.9	2.4	1	4.4	0.62	37.3	
MM10-20-12	56.8201	-131.0190	62136	73	<5	20	1000	7	35	480	3	5.32	<1	<1	<5	0.05	<50	50	6.6	34.6	<5	<0.5	<0.5	<4	80	4	<3	6	1.2	0.5	<0.5	1.4	0.06	36.6	
MM10-20-12b	56.8201	-131.0190	62137	762	16	61	300	<1	38	60	<2	10.7	2	<1	27	0.34	<50	40	5	12.9	<5	2.1	<0.5	5	110	3	5	<5	1.8	0.6	<0.5	3.6	0.57	37.1	
MM10-20-13	56.8208	-131.0201	62138	<5	<5	23	500	4	<5	60	<2	2.51	2	<1	<5	0.26	<50	<30	4.5	14.7	<5	1.8	<0.5	<4	<50	15	25	10	3.5	1.4	0.6	3.9	0.66	29.4	
MM10-22-06	56.8216	-131.0214	62139	<5	<5	5	300	<1	7	210	<2	3.26	<1	<1	<5	<0.05	<50	<30	1.9	1.5	<5	<0.5	<0.5	<4	<50	1	<3	<5	0.4	0.2	<0.5	<0.2	<0.05	39.2	
MM10-24-03	56.7598	-131.1858	62140	<5	<5	<2	1200	10	32	430	3	6.13	1	<1	<5	0.87	<50	50	2.9	35.8	<5	1.2	<0.5	<4	100	7	12	<5	1.7	0.8	<0.5	1.8	0.3	40.5	
MM10-24-04	56.7067	-131.1142	62141	413	<5	<2	1300	<1	33	110	10	7.15	2	<1	79	0.65	<50	190	0.7	14.7	<5	2	4.8	37	130	14	22	15	2.3	0.6	<0.5	2	0.26	37.5	
MM10-24-05	56.7070	-131.1141	62142	1260	8	24	500	<1	13	90	5	4.22	2	<1	29	2.49	<50	140	1	10.7	<5	3	<0.5	17	160	6	16	<5	2.3	0.7	<0.5	2	0.32	33.3	
MM10-24-06	56.6785	-131.0937	62143	675	8	206	1000	6	23	310	<2	15.1	<1	<1	180	1	<50	150	2.5	15.7	38	2.3	5.3	40	<50	16	32	<5	2.6	0.7	<0.5	1.8	0.31	36.9	
Reference Materials																																			
Standard BCS III			62144	<5	<5	75	<100	<1	58	420	<2	9.3	3	<1	<5	2	<50	<30	17.4	32.4	<5	5.9	<0.5	<4	280	30	54	20	5.8	2.6	<0.5	2.8	0.63	25	
Standard Measured			DNMAS 111	1770			1470	1200	34	50		3.03			1.9					5.9			13.9			14	25					1.7			
Standard as certified			DNMAS 111	1670			1450	1140	34	52		2.79			1.87					5.8			14			14	19.3					1.9			
Blank			BLK	<5	<5	<2	<100	<1	<5	<10	<2	<0.02	<1	<1	<5	<0.05	<50	<30	0.2	<0.1	<5	<0.5	<0.5	<4	<50	<1	<3	<5	<0.1	<0.2	<0.5	<0.2	<0.05	30	

Birthday Jim Showing

The Birthday Jim showing is located approximately 1 km north of the Dirk. Specularite skarn mineralization has been known at this locality for nearly 40 years, and was recorded during property scale mapping which extended north from the Dirk prospect (Costin, 1973). Mineralization is set in a package of southwest-striking, north-dipping volcanoclastic rocks, including coarse polyolithic volcanic conglomerate, sandstone and fine grained siltstone, cherty argillite and fossiliferous limestone. Intruding the bedded sequence are dikes and sills of fine grained pink weathering syenite and xenolith-rich biotite phyrlic syenite and a coarse potassium feldspar megacrystic syenite porphyry clast-dominated diatreme (units described previously). The syenite is locally flow laminated and displays chilled margins where it intrudes the diatreme, but where it intrudes limestone the contacts are more diffuse because the dike has assimilated limestone xenoliths and is overprinted by skarn alteration. Mineralization occurs as veins and patchy replacements of limestone xenoliths within the syenite or adjacent to the syenite contact, within limestone. Skarn mineralization is dominated by specular hematite, lesser magnetite, andradite garnet and epidote with chalcopyrite and malachite (Figures 22a, b). We collected two grab samples of specularite-chalcopyrite mineralization. Most notable of the analytical results were those obtained from sample 10JLO-182 (Table 1) which returned 0.5 % Cu, 3.8 ppm Ag and 6.4 ppm Au.

Early Carboniferous - VHMS

Verrett rhyolite

An unnamed east-flowing glacier is the northern source of Verrett River. North of this glacier is a volcano-sedimentary section comprised of well bedded rhyolite tuffite containing sulphide clasts (Figures 23a, b) and peperite sills that pass up section into rhyolite lapilli and breccia units. Preliminary U-Pb age determinations on



Figure 22a. Skarn mineralization at the Birthday Jim occurrence: photomicrograph of reflected light view of bladed specular hematite which is enclosed by late chalcopyrite. Accessory pyrite occurs outside the ~5 mm field of view.



Figure 22b. Skarn mineralization at the Birthday Jim occurrence: quartz and hematite replace colonial corals.



Figure 23a. Well bedded rhyolite tuffite with sulphide clasts.

zircons separated from this rhyolite indicate an age of ~340 Ma (the same preliminary age as determined for the rhyolite in the northeast corner of the map sheet). Sulphide veins are common within the overlying rhyolite, occurring as irregular pyrite-chalcopyrite veins in late breccia zones (Figure 23c) and as 1 to 5 cm thick, planar veins of chlorite-carbonate-euhedral pyrite ±chalcopyrite enveloped by decimetre wide carbonate alteration halos. On its western side, the succession shares a structurally modified contact with rust, tan and black turbiditic volcanic sediments. At this contact are fault-striated relicts of a barite-chalcopyrite layer up to ~5 cm thick



Figure 23b. Well bedded rhyolite tuffite is locally brecciated.



Figure 23c. Well bedded rhyolite tuffite with infillings of pyrite and lesser chalcopyrite.

(Figure 24a) at the structural base of the rhyolite tuff. Approximately 100 m above the contact with turbiditic strata the section becomes more tuffaceous with green and maroon tuffite containing magnetite-rich layers interbedded with irregular jasperoid layers (Figure 24b). Some jasperoid boulders contain stratiform layers of pyrite and chalcopyrite (Figure 24c), but chalcopyrite layers could not be found in place.

Barite, chalcopyrite, magnetite layers and jasper layers are all features of productive VMS environments. If the Fe-rich tuff – jasper layers are exhalative in origin, they represent active subaqueous hydrothermal environment in which chalcopyrite is accumulating, and significant mineral exploration target. Jasperoid layers within the stratigraphy about 1.5 km to the southeast may be related and, if so, represents a target with significant strike length.

Andrei rhyolite

Perhaps the most inconspicuous mineralization encountered during the 2010 mapping campaign shows no sign of having been looked at previously. Mineralization occurs in a section of felsic flows and tuff, pillowed mafic flows and hyaloclastite, and immature volcanic sediments

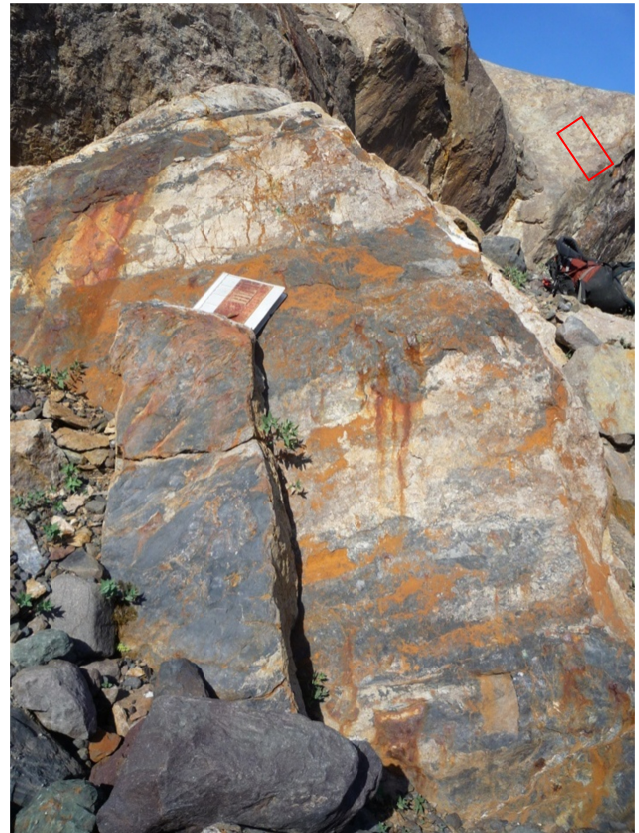


Figure 24a. The structurally modified contact between fine grained turbiditic sediments and coarse rhyolite tuff is a layer of baritic argillite with chalcopyrite (inset).



Figure 24b. Stratigraphically above the turbiditic section is well-bedded tuffite with magnetite-rich layers as well as jasperoid layers.

in the northeast part of the map area. An early Carboniferous age is indicated by extension of geology mapped by (Logan *et al.*, 2000) as well as a new preliminary isotopic age determination of ~340 Ma. Mineralization consists of finely disseminated chalcopyrite and millimetre to centimetre clots of covellite-bornite as intergrowths with mafic glomerocrysts or xenoliths (?) in a medium grained K-feldspar-phyric unit (Figures 25a, b). Millimetre-thick, black, irregular quartz veinlets locally cut the unit. Copper



Figure 24c. Boulders of jasper contain stratiform pyrite and, as seen here, chalcopyrite.



Figure 25a. Character of black veinlets cutting a typical exposure of the Andrei rhyolite. Metal content is related to disseminated sulphides as contents determined by analyses remain consistent regardless of the degree of veining.

staining is scarce. We interpret the unit as a rhyolite flow and flow breccia unit, but it could be a dike with highly irregular margins. Two samples of this unit were collected about 10 m apart, both contain appreciable Cu (1600 ppm), Zn (4000 ppm), Ag (5.8 ppm) and Cd (14 ppm; see Table 1 and note consistency of replicate analyses). In consideration of its potentially consistent but inconspicuous mineralization, this unit and others like it need to be systematically mapped and sampled.

Pink epidote veins

On the ridge east of Twin Glacier, pink veins composed of a resistant, hard silicate mineral cut the ~187 Ma hornblende ±biotite dacite ash flow / air fall tuff and breccia. Such veins may be of interest to mineral collectors and more than ten of these veins occur within a zone that extends at least 100 m and may be 30 m across. Individual veins attain thicknesses of 0.5 m but pinch and swell, such that 5-10 cm thickness is more typical (Figure 26). Petrographic analysis of one of the vein samples collected reveals a fine grained intergrowth of quartz with

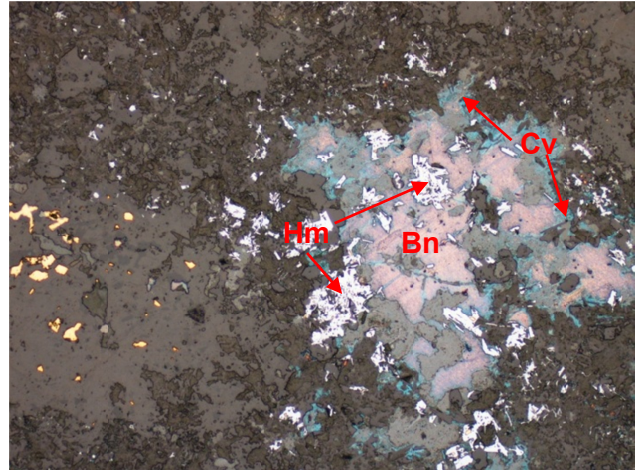


Figure 25b. Photomicrograph of mineralization within mafic clots in the felsic volcanic unit includes purple twinned bornite (Bn) rimmed by pleochroic blue covellite (Cv) and enclosing idiomorphic blue-white hematite (Hm). Disseminated chalcopyrite occurs outside the ~1.2 mm field of view. Disseminations of a yellow, highly reflective mineral at the left centre have a softer polishing hardness and higher reflectance than is typical of chalcopyrite (perhaps cubanite or eskebornite, CuFeSe_2). Sphalerite occurs as ~20-30 μ irregular blebs scattered around the margins of the bornite.



Figure 26. Veins of pink epidote cut feldspar-phyric volcanic rocks east of Twin Glacier.

minor carbonate and chlorite and a predominance of a strongly zoned, high relief, highly birefringent mineral (~0.035) with yellow-lime to pale pink pleochroism. Optical properties, confirmed by XRD analysis, indicate that the mineral is epidote, probably a Mn-bearing

pistacite, as opposed to the optically positive and strongly pleochroic (magenta to yellow) piedmontite, the Mn-rich member of the epidote family. Trace element analysis of the vein reveals only minor Mn-enrichment (which may impart the pale pink colour), but relatively high values of hafnium and zirconium (0.19 and 6.3 ppm, see Hf and Zr, sample MMI10-13-7, Table 1).

STRUCTURAL GEOLOGY

Zones of foliated, folded and faulted rocks have been identified at various scales throughout the map area. However, the strongest penetrative fabrics affecting areas of more than a square kilometre are generally restricted to the regions south and west of the Twin River pluton where two phases of folding are displayed.

Folds, foliation and schistosity

Partitioning of strain into elongate, foliated domains can be observed on the ridges east of Twin Glacier. Some of these domains can be explained by their position in the axial zones of mainly northwest-trending folds. Northeast-verging thrusts and duplex zones which are presumably syn-kinematic with northwest-trending folds, are interpreted to root beneath the foliated rocks.

On the nunatak between the Twin Glaciers, penetrative fabrics are developed in the volcano-sedimentary rocks. In these areas, the rocks are pervasively recrystallized to such an extent that they are locally schistose. Strong to moderately strong, steep S1 foliation is shallower than or sub-parallel to poorly preserved bedding indicating local upright isoclinal folding of the stratigraphy. S1 is commonly accompanied by development of strong to intense, steep to downdip stretching lineation, locally with L>S, forming L-tectonites. L-tectonites are spectacularly preserved in limestone-bearing conglomerates where the limestone clasts have aspect ratios of $\gg 10:1$. S1 is overprinted by open to tight recumbent F2 folds with minimal S2 development.

Timing and conditions leading to the formation of the schistosity have not been firmly established. North and east of the map area Logan and Koyanagi (1994) and Logan *et al.* (2000, Figure 2; 1994) record similar fabrics which affect pre-mid Carboniferous rocks; whereas the strata affected at Twin Glacier nunatak are suspected to be Triassic (Kerr, 1935; Fillipone and Ross, 1989). Age control for strata at the nunatak are lacking and interleaving of foliated and non-foliated strata by complex thrust faulting cannot be ruled out. Minimum age of D1 is constrained as pre-Eocene, the age of the Twin River pluton that appears to hornfels the S1-L1 tectonites. The age of S2 is not constrained as the hornfelsed Triassic strata do not appear to preserve F2.

Some schistose fabrics were developed in response to intrusion of the Twin River pluton, but these fabrics are restricted to a zone within ~500 m of the pluton contacts. Elsewhere, fabrics within regionally foliated rock

outcrops are cut by the pluton and related dikes. At the map scale, regional foliation tends to wrap around the margin of the intrusion. Such relations suggest that pluton emplacement was in part accommodated by ductile flow of country rocks.

Folds and thrust belts

Thrust faults are best displayed within well bedded, relatively incompetent strata which presumably acted as glide horizons and décollements. This strain is particularly concentrated within two units: sooty and cherty strata of presumed Middle Triassic age and chert-claystone of presumed Carboniferous age. Nevertheless, well bedded calcareous wacke has also been deformed by thrust faulting; and thrust offsets within this unit must be appreciable as a several hundred metre-long zone of complex, thrust-related deformation has been developed ~3 km east of Twin Glacier (Figures 27a, b). Fold asymmetry within both the footwall and hangingwall, as well as the geometry of bedding cut-offs, suggest that thrusts mainly verged to the north and east.



Figure 27a. A cliff face between the clouds east of Twin Glacier displays an incised thrust belt.

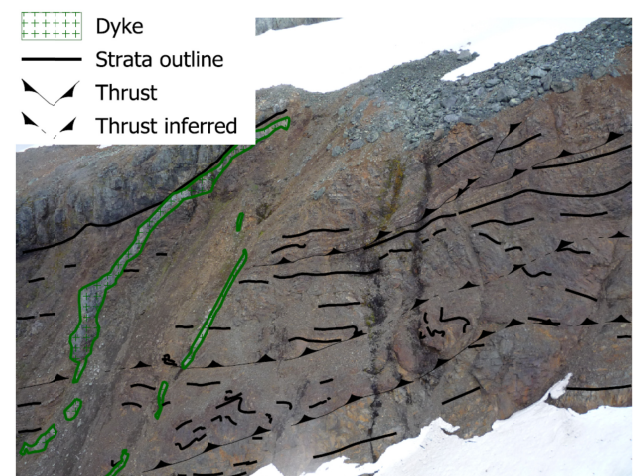


Figure 27b. An interpretation of the deformation displayed by the strata.

Late faults

Two major brittle-ductile faults have been mapped. The apparent offsets on these faults are inferred to exceed 1 km, and as such they impart a significant control on the continuation of stratigraphic units and mineralization. The faults are named after nearby geographic features: Andrei Glacier fault and the Verrett-Iskut Fault.

Andrei Glacier fault

Numerous fault strands that together comprise the Andrei Glacier Fault are exposed and oriented northwest, roughly parallel to the northeastern margin of the Andrei Glacier. This fault juxtaposes Middle Carboniferous carbonate (Logan *et al.*, 2000) to the northeast, with orange-weathering conglomerate of presumed Late Triassic age to the southwest. Orange, strongly carbonate-altered, 1 to 2 m thick dikes have intruded along the fault zone where they display ghosted, coarse phenocrysts that are probably relicts of orthoclase. Similar dikes are observed cutting Triassic strata to the south and are interpreted to be of Late Triassic age.

Several sets of minor structures have been identified within the fault zone including two sets slickensides indicating components of subhorizontal-dextral as well as south-side-down-normal motion. We acknowledge that the slickensides are minor features that may have formed at any time, even in response to glacial rebound. However, the downdip slickensides are superimposed on fault flutings with ~10 cm of relief and may represent significant fault motion. The entire Upper Carboniferous and most of the Late Triassic section appears to be offset across the fault, perhaps as much as 3 km of apparent vertical displacement. Actual offset could be much less depending upon how much section was removed during a sub-Late Triassic erosional event.

The opposite sense of relative offset is displayed by the inferred northwest extensions of the Andrei Glacier fault where polymictic conglomerate of presumed Upper Triassic age that lay northeast of the fault is juxtaposed with Early Permian strata southwest of the fault. Thus, motion on the fault may have been either scissor-like or the fault displaced previously deformed strata (*e.g.*, folded strata). Southeast extensions of the Andrei Fault are orthogonal to the northeast-trending McLymont fault and other faults bounding the Newmont Lake graben (Logan *et al.*, 2000), suggesting that the Andrei Glacier Fault predates the Newmont Lake Graben.

Verrett-Iskut fault

The Verrett-Iskut fault (V-I fault) is a discrete, high angle fault with a gently arcuate ~east-trending trace. On the southeast flank of Mount Verrett, the V-I fault cuts off a Paleozoic marble unit that is ~200 to ~450 m thick. One kilometre north of the fault, relict layering within the marble dips moderately west. Nearer the fault, layering steepens. Based upon its map pattern, the marble is nearly vertical where intersected by the VI fault. South of the

fault and to the east in 104B/15 (Logan *et al.*, 2000), a band of marble outcrops can be extrapolated to intersect the fault at a point which would indicate ~1800 m of sinistral offset. If the marble is vertical where cut by the fault, the 1800 m of apparent sinistral offset is likely close to the true horizontal component of offset.

Farther east, the VI fault juxtaposes Late Devonian biotite granite and Devono-Mississippian tuffaceous rocks in 104B/15 (Logan *et al.*, 2000). To the west, the V-I fault appears to follow a well-defined, glacially scoured lineament trending ~250°, until it is lost at elevations below 1200 m. In this area, adjacent units of “quartz sandstone” and mafic tuff with a combined thickness of 300-500 m and enveloped by argillite are also offset by the fault (see Figure 2 and Mihalyuk *et al.* 2011 for data sources). Amount of offset cannot be precisely constrained because the unit contacts are not exposed, but about 1450 m of apparent sinistral motion is indicated.

WHERE DOES THE WESTERN V-I FAULT GO (?)

West of its intersection with the Iskut River valley bottom, the VI fault is masked by the vegetation and Quaternary sediments. However, the VI fault is unlikely to trend directly west across the Iskut River because it does not offset a belt of limestone between the Craig and Iskut rivers (see Figure 3). Instead, it is interpreted to deflect northwest-ward towards the “Sulphide Ridge” and the Rock and Roll deposit (Figure 3). Farther west, the most likely fault trace beyond its point of re-emergence from the river gravels is obscured by Quaternary to Recent lava flows of Hoodoo Mountain, or by the Hoodoo River alluvial fan deposits. Strong magnetic susceptibility of the flows and clay-rich layers in the gravels obscure both aeromagnetic and airborne electromagnetic responses on geophysical surveys reported by Jones (2009), Walcott, (2009) and Dvorak (1991). However, a

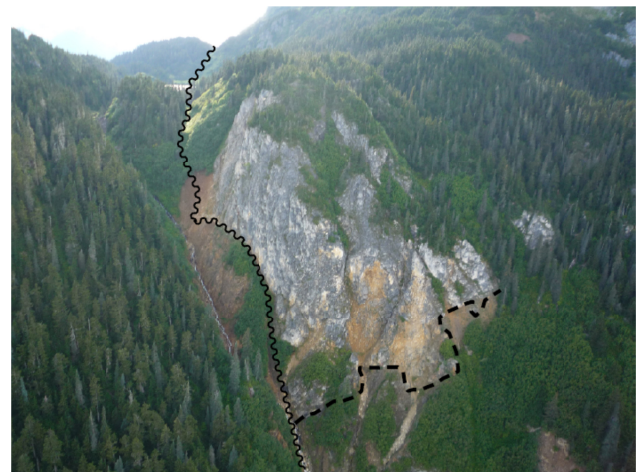


Figure 28. A view to the west along the Verrett-Iskut fault on the southeast flank of Mount Verrett (photo taken from above Verrett River). Following the V-I fault is a strong topographic lineament. A highly irregular trace of the eastern marble contact (highlighted by dashed line) is interpreted as due to intersection of a subvertical contact surface with the steep topography. In the upper right corner of the photo is the northern continuation of the marble band.

break in the aeromagnetic responses in the survey reported by Jones (2009) may respond to a fault trace B on Figure 3 that is deflected slightly to the north. Minimal deflection of the fault is shown by the fault trace A option.

HOW MUCH OFFSET ON V-I FAULT (?)

The displacements of marble bands and quartzose sandstone indicate an average sinistral offset of ~1600 m in the eastern part of the Iskut River valley. Alternatively, decreasing sinistral offset along the fault to the west, as could be inferred from the data, may result in westward decrease of apparent motion by as much as 350 m per 5 km. Hence, the northern continuation of the “Sulphide ridge” stratigraphy could intersect the fault about 10 km west of the offset quartz-rich sandstone. At this point ~750 m of apparent sinistral offset might be inferred. Constraints on the vertical component of motion on the fault are lacking.

WHERE IS THE NORTHERN ROCK AND ROLL (?)

Modelled offsets and locations of the western V-I fault extension have significant implications for identification of a northern continuation of the strata that host the Rock and Roll deposit. Before speculating on the continuation of the Rock and Roll host strata north of the Iskut River Valley, it is necessary to consider several caveats:

- 1) The mineralization at the Rock and Roll deposit may not have a northern extension. Although the Rock and Roll deposit appears to be stratiform, a syngenetic origin has yet to be unequivocally established (*e.g.* Mihalyuk *et al.*, 2010). Even if the mineralization is stratiform, it may not have had sufficient lateral continuity to outcrop to the north.
- 2) A northwestern extension of Rock and Roll, if it ever existed, may have been located above the present erosional surface unless the folds that deform the prospective stratigraphy remain approximately horizontal on average or plunge northwestward.
- 3) Units on “Sulphide Ridge” while complexly folded, display relatively simple bounding surfaces and intersection of these bounding surfaces with present day topography have a relatively consistent northwest trend. In this analysis it is assumed that this trend persists beyond the V-I fault extension.

In the simplest case scenario, barring any of the complication noted above, a potential extension to the Rock and Roll mineralization could be somewhere between the two localities marked by the thick blue and red lines on Figure 3. This supposition needs to be tested by constraining the location of carbonate belt north of the VI fault, particularly because the axis of mineralization

along “Sulphide ridge” is consistently between 350 and 450 m northeast of this contact.

SUMMARY

Parts of the southern Hoodoo Mountain sheet were first mapped at a reconnaissance scale by Forrest Kerr between 1926 and 1929. Yet, despite the high mineral potential of the adjacent areas, the northern 2/3 of the sheet was never systematically mapped prior to the work presented here. This report is a synopsis of 2.5 weeks of intensive field investigation that established a geological framework for the eastern Hoodoo Mountain sheet, and extended that framework southwards into the Iskut River valley, where a wealth of geological data exists in industry reports.

Our mapping revealed that the regional geological contacts formerly extrapolated through the Hoodoo Mountain area (Massey *et al.*, 2005) inadequately represent its geological complexity and high mineral potential. As a result, significant mineral prospects, such as the Dirk, which has been recognized since at least 1972, lacked regional geological framework around which a district exploration program could be established.

Even though our mapping was limited by budgetary constraints, it provides enough detail for first order predictive metallogeny, and directions for future mineral exploration work. For example:

- Modelled offset on the V-I fault provides an exploration target for the northern extension of strata that host the Rock and Roll deposit. Future work should include detailed structural analyses aimed at constraining the displacement on units in the western Hoodoo Mountain area, including the vertical component of motion on the V-I fault.
- Recognition of a corridor of alkalic intrusive/volcanic “centres” permits us to pose the question of how extensive are mineralizing systems within the corridor? Alkalic rocks hosting mineralization at the Dirk are analogous to mineralizing intrusions at the Galore Creek deposit. Future work should address characteristics specific to mineralizing intrusions and their extents within the corridor.
- Our work outlines a bimodal submarine volcanic succession of Carboniferous age that contains indications of an active VMS mineralizing system of regional extent. Future exploration work will need to evaluate the significance and distribution of newly discovered primary Cu-Ag-Zn mineralization in both the Andrei rhyolite and the Verrett Creek rhyolite separated by ~20 km.

We will attempt to address some of these questions with targeted laboratory work, but others await the future work of explorationists and regional mappers in the eastern Hoodoo Mountain area. Some answers may lie in

the western Hoodoo Mountain area, parts of which STILL lack regional geological mapping.

ACKNOWLEDGMENTS

This project would not have been possible without the financial assistance of our project partners: Pacific Northwest Capital, the Geological Survey of Canada GEM initiative, and the University of Victoria (British Columbia Ministry of Energy, Mines and Resources Partnership Fund). This project is also funded in part by an NSERC Discovery grant to Stephen T. Johnston. Safe and courteous helicopter support was provided by Jim Beise of VIH Helicopters Ltd. Renaud Soucy la Roche ably assisted with field work. Comfortable accommodations were arranged by David Jensen and others of Skyline Gold Corp. We are especially grateful for the excellent camp cuisine and maintenance all attributable to Esther Nagli of Rugged Edge Holdings Ltd.

REFERENCES

- Anderson, R.G. (1993): A Mesozoic stratigraphic and plutonic framework for northwestern Stikinia (Iskut River area), northwestern British Columbia, Canada; in *Mesozoic Paleogeography of the Western United States - II*, Dunne, G. and McDougall, K. (Editors), *Society of Economic Paleontologists and Mineralogists, Pacific Section*, 71, pages 477-494.
- BC MINFILE (2010): British Columbia mineral inventory database; *BC Ministry of Energy, Mines and Petroleum Resources*, online database, <http://www.empr.gov.bc.ca/MINING/GEOSCIENCE/MINFILE/Pages/default.aspx> [November, 2010].
- Bernales, S., Chadwick, P. And Guszowaty, E. (2008): 2008 exploration activities on the Romios Gold Resources, Inc. Newmont project, prepared for Romios Gold Resources; *B.C. Ministry of Energy, Mines and Petroleum Resources*, Assessment Report 30449, 59 pages plus 12 appendices.
- Britton, J.M., Fletcher, B.A. and Alldrick, D.J. (1990): Snippaker map area (104B/6E, 10W, 11E); in *Geological Fieldwork 1989*, *BC Ministry of Energy, Mines and Petroleum Resources*, Paper 1990-1, pages 115-125.
- Brown, D.A., Gunning, M.H. and Greig, C.J. (1996): The Stikine Project: Geology of western Telegraph Creek map area, northwestern British Columbia (NTS 104G/5,6,11W, 12 and 13); *BC Ministry of Employment and Investment*, Bulletin 95, 175 pages.
- Brown, D.A., Logan, J.M., Gunning, M.H., Orchard, M.I. and Bamber, W.E. (1991): Stratigraphic evolution of the Paleozoic Stikine assemblage in the Stikine and Iskut Rivers area, northwestern British Columbia; *Canadian Journal of Earth Sciences*, Volume 28, pages 958-972.
- Chadwick, P. and Close, S. (2009): Geological and geochemical report on the Dirk property, prepared for Romios Gold Resources; *B.C. Ministry of Energy, Mines and Petroleum Resources*, Assessment Report 31250, 31 pages plus appendices.
- Clothier (1918): The Stikine Mining Division-Iskut Mining camp; *BC Minister of Mines*, Annual Report of the Minister of Mines for 1917, pages 73-74.
- Cohoon, G.A. and Trebilcock, D.A. (2004a): Phiz Property geology and geochemistry surveys; *BC Ministry of Energy, Mines and Petroleum Resources*, Assessment Report 27555, 73 pages plus appendices and maps.
- Cohoon, G.A. and Trebilcock, D.A. (2004b): Rock and Roll Project, Geology and Geochemical Surveys; *BC Ministry of Energy, Mines and Petroleum Resources*, Assessment Report 27582, 84 pages plus maps.
- Costin, C.P. (1973): Report of geological, geophysical, and physical work, Dirk claim group; *BC Ministry of Energy, Mines and Petroleum Resources*, Assessment Report 4150, 15 pages plus maps.
- Dvorak, Z. (1991): Geophysical Report on the Hard Place Project; *BC Ministry of Energy, Mines and Petroleum Resources*, Assessment Report 21681, 27 pages.
- Edwards, B.R., Anderson, R.G., Russell, J.K., Hastings, N.L. and Guo, Y.T. (2000): The Quaternary Hoodoo Mountain Volcanic Complex and Paleozoic and Mesozoic basement rocks, parts of Hoodoo Mountain (NTS 104B/14) and Craig River (NTS 104B/11) map areas, northwestern British Columbia, *Geological Survey of Canada*, Open File 3721, scale 1:20 000.
- Fillipone, J.A. and Ross, J.V. (1989): Stratigraphy and structure in the Twin Glacier-Hoodoo Mountain area, northwestern British Columbia (104B/ 14); in *Geological fieldwork 1988*, Smyth (Editor), *BC Ministry of Energy, Mines and Petroleum Resources*, 1989-1, pages 285-292.
- Gifford, R.G. (1980): Geological report – Inel mineral claims; *BC Ministry of Energy, Mines and Petroleum Resources*, Assessment Report 8997, 10 pages, 3 appendices and 4 maps.
- Gunning, M.H., Bamber, E.W., Brown, D.A., Rui, L., Mamet, B.L. and Orchard, M.J. (1994): The Permian Ambition Formation of northwestern Stikinia, British Columbia; in *Pangaea; global environments and resources*, Embry, F, Beauchamp, B and Glass (Editors), *Canadian Society of Petroleum Geologists*, 17, pages 589-619.
- Harland, W.B., Armstrong, R.L., Cox, A.V., Craig, L.E., Smith, A.G. and Smith, D.G. (1990): *A Geological Time Scale 1989*; Cambridge, Cambridge University Press.
- Jones, M. (2009): 2009 Geophysical Report on the Rock and Roll Property; *BC Ministry of Energy, Mines and Petroleum Resources*, Assessment Report 31158, 59 plus geophysical maps pages.
- Kerr, F.A. (1935): Stikine River Area, South Sheet, Cassiar District, British Columbia; *Geological Survey of Canada*, Map 311A, 1:126 720 scale.
- Kerr, F.A. (1948): Lower Stikine and western Iskut River areas, British Columbia; *Geological Survey of Canada*, Memoir 246, 94 pages.
- King, G.R. (1987): Geological and geochemical report on the Ian 1 to 4 claims, Iskut River area, Liard mining division, B.C. *BC Ministry of Energy, Mines and Petroleum Resources*, Assessment Report 16953, 19 pages plus 6 appendices and 4 maps.
- Lefebvre, D.V. and Gunning, M.H. (1989): Geology of the Bronson Creek area, NTS 104B/10W, 11E [in part]; *BC Ministry of Energy, Mines and Petroleum Resources*, Open File 1989-28, 2 sheets, 1:25 000 scale.

- Lewis, P.D., Mortensen, J.K., Childe, F., Friedman, R.M., Gabites, J., Ghosh, D. and Bevier, M.L. (2001): Geochronology data set; Metallogenesis of the Iskut River area, northwestern BC, *Mineral Deposits Research Unit*, Miscellaneous Report, pages 89-96.
- Logan, J.M. (2004): Preliminary lithogeochemistry and polymetallic VHMS mineralization in Early Devonian and (?) Early Carboniferous volcanic rocks, Foremore property; in *Geological fieldwork 2003, BC Ministry of Energy, Mines and Petroleum Resources*, Paper 2004-1, pages 105-124.
- Logan, J.M. and Koyanagi, V.M. (1994): Geology and mineral deposits of the Galore Creek area (104G/3, 4); *BC Ministry of Energy, Mines and Petroleum Resources*, Bulletin 92, 96 pages.
- Logan, J.M., Drobe, J.R. and McClelland, W.C. (2000): Geology of the Forrest Kerr-Mess Creek Area, Northwestern British Columbia (NTS 104B/10, 15 & 104G/2 & 7W); *BC Ministry of Energy, Mines and Petroleum Resources*, Bulletin 104, 163 pages.
- Macrae, R., and Hall, B.V. (1983): Geological and geochemical report on the Hemlo west and Aurum claim group, Iskut River area, Liard Mining Division, *BC Ministry of Energy, Mines and Petroleum Resources*, Assessment Report 11320, 24 pages plus 4 appendices and 9 maps.
- Massey, N.W.D., MacIntyre, D.G., Desjardins, P.J. and Cooney, R.T. (2005): Digital Geology Map of British Columbia: Whole Province, *BC Ministry of Energy, Mines and Petroleum Resources*, Geofile 2005-1.
- Mihalynuk, M.G., Stier, T.J., Jones, M.I. and Johnston, S.T. (2010): Stratigraphic and structural setting of the Rock and Roll deposit, northwestern British Columbia; in *Geological Fieldwork 2009, BC Ministry of Energy, Mines and Petroleum Resources*, Paper 2010-1, pages 7-18.
- Mihalynuk, M.G., Logan, J.M. and Zagorevski, A. (2011a): East Hoodoo Mountain - Iskut River Geology (NTS 104B/14E, 11NE); *BC Ministry of Energy, Mines and Petroleum Resources*, Open File 2011-4, 1:50 000 scale map.
- Mihalynuk, M.G., Logan, J.M. and Zagorevski, A. (2011b): Tabulated digital geochemical results from samples collected in the East Hoodoo – Iskut River area (NTS 104B/14E, 11NE); *BC Ministry of Energy, Mines and Petroleum Resources*, Geofile 2011-1, on-line.
- Monger, J.W.H. (1977): Upper Paleozoic rocks of the western Canadian Cordillera and their bearing on Cordilleran evolution; *Canadian Journal of Earth Sciences*, Volume 14, pages 1832-1859.
- Montgomery, A.T., Todoruk, S.L. and Ikona, C.K. (1991a): Assessment Report on the Rock and Roll Project; *BC Ministry of Energy, Mines and Petroleum Resources*, Assessment Report 20884, 18 pages plus figures, appendices and maps.
- Montgomery, A.T., Todoruk, S.L. and Ikona, C.K. (1991b): 1990 Summary geological and geochemical report on the STU 8 & 9 mineral claims, Liard Mining Division; *BC Ministry of Energy, Mines and Petroleum Resources*, Assessment Report 21051, 15 pages plus figures, 8 appendices and 5 maps.
- Mortensen, J.K., Gosh, D. and Ferri, F. (1995): U-Pb geochronology of intrusive rocks associated with Cu-Au porphyry deposits in the Canadian Cordillera; in *Porphyry deposits of the northwestern Cordillera of North America*, in Schroeter, T. G. (Editor), *Canadian Institute of Mining and Metallurgy*, Special Volume 46, pages 142-158.
- Okulitch, A.V. (1999): Geological time scale, 1999; *Geological Survey of Canada*, National Earth Science Series, Geological Atlas, Open File 3040, wall chart.
- Pegg, R. (1989): Geological and Geochemical Report on the 1989 Exploration Program of the Rock and Roll property; *BC Ministry of Energy, Mines and Petroleum Resources*, Assessment Report 19566, 8 pages plus 8 appendices and 5 maps.
- Ray, G.E. (2006): Geology, mineral potential & 2005 work completed at the Romios Gold Resources property, McLymont Creek Forrest Kerr area, NW British Columbia; *BC Ministry of Energy, Mines and Petroleum Resources*, Assessment Report 29085, 189 pages.
- Rhys, D.A. (2000): Geology and metallogeny of the Johnny Mountain area; in *Metallogenesis of the Iskut River area, northwestern B.C.*, *Mineral Deposit Research Unit*, Special Publication Number 1, pages 300-324.
- Souther, J.G. (1971): Geology and mineral deposits of Tulsequah map-area, British Columbia; *Geological Survey of Canada*, Memoir, 362, 84 pages.
- Walcott, P.E. (2009): Geophysical Interpretation Report on the Grizz and Zip Properties, Assessment Report 30936, 86 pages plus maps.
- Woodsworth, G.J., Anderson, R.G., Armstrong, R.L., Struik, L.C. and Van der Heyden, P. (1992): Plutonic regimes; in *Geology of the Cordilleran Orogen in Canada*, Gabrielse, H. and Yorath, C. J. (Editors), *Geological Survey of Canada*, Geology of Canada, No. 4, pages 493-531.

